chemosensors

MDPI

Review

Amino Acid-Functionalized AuNPs and AgNPs as Probes for the Selective Detection of Heavy Metals in the Environment

Roqaya Mohamed Elnagar [1], Gul Shahzada Khan [1,*], Irshad Ul Haq Bhat [1], Suad Ahmed Rashdan [1,*] and Awal Noor [2,*]

[1] Department of Chemistry, College of Science, University of Bahrain, Sakhir 32038, Bahrain
[2] Department of Chemistry, College of Science, King Faisal University, Al-Ahsa 31982, Saudi Arabia
* Correspondence: gkhan@uob.edu.bh (G.S.K.); srashdan@uob.edu.bh (S.A.R.); anoor@kfu.edu.sa (A.N.)

Abstract

The literature collected from various search engines and high-quality scientific databases reveals that amino acid (AA)-functionalized nanoparticles have emerged as a promising field for selective detection and remediation of heavy metals (HMs). Among the various nanoparticles (NPs), gold nanoparticles (AuNPs) and silver nanoparticles (AgNPs) have drawn considerable attention, attributed to their unique optical, catalytic, and surface plasmon resonance properties. Functionalization with amino acids significantly enhances nanoparticle stability, biocompatibility, and metal-binding affinity through diverse functional groups. AA-functionalized AuNPs, including glycine, cystine, leucine, methionine, tyrosine, aspartic acid, histidine, and lysine-capped systems, exhibit tunable selectivity toward heavy metal ions. Bifunctionalization strategies further enhance sensitivity by inducing nanoparticle aggregation or signal amplification. Beyond single amino acids, polypeptides and protein-functionalized AuNPs offer enhanced molecular recognition and multivalent binding, expanding their applicability in complex matrices. Similarly, amino acid-functionalized AgNPs, such as those capped with similar amino acids stated above, exhibit strong interactions with heavy metals, AA bifunctionalization, and bimetallic nanoparticles (BNPs), particularly amino acid-functionalized Au–Ag systems, which combine the advantages of both metals, leading to improved sensitivity, selectivity, and signal strength. Although these advances have been made, a major gap remains in the systematic comparison of different amino acids, peptides, and bimetallic systems under real-world conditions. This gap can be addressed by standardized testing methods, clearer structure–function relationships and combined experimentation to guide the rational design of more efficient AA-functionalized nanoparticles.

Keywords: AuNPs; AgNPs; heavy metals; amino acid; detection; biosensors; environmental monitoring

Check for updates

Received: 27 March 2026
Revised: 7 May 2026
Accepted: 12 May 2026
Published: 14 May 2026

Copyright: © 2026 by the authors. Licensee MDPI, Basel, Switzerland. This article is an open access article distributed under the terms and conditions of the Creative Commons Attribution (CC BY) license.

1. Introduction

Heavy metals (HMs) are naturally present in the environment [1], and an increase in their abundance is attributed to anthropogenic activities [2]. Geological events, including volcanic eruptions and erosions [3], also contribute to their undesired concentration in the natural environment. HMs exist in the environment as cations, i.e., Cd(II), Mn(II), Hg(II), Ni(II), Zn(II), etc. [1,4]. HMs accumulate in the soil and combine with organic and inorganic contents, increasing the soil toxicity profile [5]. This phenomenon leads to the transport of HMs into water bodies. The bioavailability of HMs in soil and water poses a

significant threat to living organisms, causing long-term DNA alterations and death due to their intrinsic cytotoxicity [6]. Sorption of HM ions on sediments, organic and inorganic ligands, explains the mobility and persistence of these ions. In addition to the precipitation of metals (as metal sulfates, carbonates, hydroxides, or hydrogen phosphates), microbial activities, chemical compounds in sediments, and the methylation of some metals influence the oxidation and reduction in metals [1,4]. The presence of undesired HMs in different environmental compartments poses a serious threat to environmental sustainability due to their non-biodegradable and bioaccumulative properties [7]. The high mobility of these metals increases their bioavailability and results in serious environmental impacts [1,4].

Thus, accurate detection of HMs is crucial to ascertaining pollution problems. It is important to address the gap for developing and refining the detection methods to remove HMs from the environment. The detection methods widely used for HMs include inductively coupled plasma mass spectrometry/atomic emission spectrometer, atomic absorption spectrometry, atomic fluorescence spectrometry, laser-induced breakdown spectrometry and atmospheric pressure discharge plasma technology [8]. In addition, neutron activation analysis and X-ray fluorescence techniques have shown high efficiency and accurate evaluation capabilities [9]. Among the latest emerging technologies, chemical and optical nanosensors stand out as among the most effective systems for detecting toxic HMs, with enhanced detection limits, quantification capabilities, and ease of on-site operation [10]. Moreover, biomaterials, advanced polymers, functional nanomaterials, and porous materials are also used in the effective detection and elimination of HMs. Such systems are appreciated not only for their real-time detection, high removal efficiency, quick response, and low detection limits but also for their resistance to interference, excellent selectivity, and robust performance [11].

Enhancing the sensitivity of analytic techniques constitutes emerging technologies such as the use of nanomaterials, which can be used for preconcentration, increasing the sensitivity of the analytical technique and allowing real quantification of the sample. The electrochemical methods, which are cost-effective, less time-consuming, and user-friendly, provide the best in-field application alternative, offering fast response and high sensitivity. The accurate detection and application of appropriate remedial techniques are vital due to the toxic, non-biodegradable nature of HMs and their bioaccumulation in the food web [12]. Conventional heavy metal remediation methods, such as chelation, coagulation, and ion exchange, often require large amounts of chemicals and can cause secondary pollution. As a result, recent research has increasingly focused on nanomaterials as cleaner and more effective alternatives for heavy metal detection and remediation [2,6,7].

Metal nanoparticles (NPs) demonstrate unique physicochemical properties owing to their small size and high surface area [13]. Metal nanoparticles (MNPs), especially Au and AgNPs, improve the selectivity and sensitivity of analytical techniques, such as colorimetric and electrochemical sensors. Their unique properties improve the limit of detection for heavy metals [14]. However, the use of metal-based nanoparticles also has limitations, with respect to biomedical and environmental hazards [15–17]. The employment of biocompatible ligands and systematic functionalization not only improves the qualities of metal nanoparticles, i.e., AuNPs, but will also minimize their toxicity. Dispersion retention and prevention of aggregation in biological environments can be achieved with the right stabilizing agents and surface coatings. The modification to enhance biocompatibility and targeted delivery can reduce associated health risks and accelerate clearance [15]. The design of NPs such as AuNPs and AgNPs with molecules of biological origin, i.e., amino acids (AAs), could be incorporated [18]. The high binding energies of deprotonated AAs to the NPs imply that AAs play a significant role in the synthesis and stabilization of NPs in different pH media. The ability to interact efficiently with metal ions and stabilize

NPs makes AA-functionalized AuNPs and AgNPs suitable for biosensing and biocatalytic applications [19]. Despite significant recent advances, the main research gap lies in the lack of systematic comparative studies correlating amino acid structure, binding mechanisms, and real-sample performance across mono/bimetallic nanoparticle systems. This gap can be addressed by integrating experimental sensing platforms with testing practices and application-oriented validation in environmental and biological samples, thereby enabling the rational design of novel and next-generation AA-functionalized nanomaterials.

1.1. Benefits of AA-Functionalized NPs

Amino acid-functionalized AuNPs and AgNPs have better stability. For example, the cysteine thiol and histidine imidazole moieties in AAs help in binding to the NPs, thus stabilizing functionalization. Moreover, the surface functionalization provides additional sites, such as amino- or carboxyl groups [20]. Amino acid-functionalized AuNPs have better selectivity and sensitivity of colorimetric sensors toward toxic metal ions. The functionalities in AAs are complex with metal ions and interact with the AuNPs. Such a process may either promote or inhibit the aggregation of AuNPs in the presence of metal ions, which is the most notable aspect that gives rise to color changes, thereby promoting naked-eye-based discrimination among metal ions. Notably, AAs such as lysine, histidine, cysteine, tyrosine, and arginine impart selectivity to the sensor array through several mechanisms of interaction with the AuNPs and the metal ions. Rightly regulating the agglomeration of AuNPs increases the colorimetrical response, thus allowing the recognition of various toxic metal ions in aqueous media [21]. Amino acid-based functionalized materials offer benefits in detection and sensing applications due to their structural variations in the side chains. AA-based materials have lower toxicity, biodegradability and biocompatibilities. The diversity of functional groups on the side chain also provides stable conformations during complexation with a variety of metal cations in aqueous environments. AAs can also be used or modified to polymeric form on their own and can be integrated with other polymeric materials as a membrane coating for enhanced selectivity. Despite the various environmental benefits of AA-functionalized materials, their large-scale applications have to be carefully evaluated and monitored in real-world applications for HM detection and applications [22].

The effectiveness of EDTA in removing HMs does not alleviate concerns about non-degradable EDTA residues, which can adversely affect normal biochemical processes. Additionally, the efficiency of HM adsorption by EDTA decreases due to the non-selective complexes EDTA forms with essential soil elements, including K, Ca, and Mg [2,23]. In comparison, AAs form stable chelates with various metal ions through their distinct side groups, varying in size, form, charge properties, ability to form hydrogen bonds, and chemical interactions. Moreover, modified AAs are effective HM chelators, as they can selectively interact with the metal ions in environments, facilitating their removal. This effectiveness can be attributed to the selectivity and greater competitiveness of AAs compared to EDTA [24].

This review aims to investigate the effectiveness of AA-functionalized materials in the detection and elimination of HMs from contaminated environments. This review provides a comprehensive overview of amino acid-functionalized Au and Ag NPs. This review seeks to evaluate the potential of various innovative materials in enhancing the adsorption capacity, selectivity, and efficiency of HM removal by reviewing the latest developments in this field. It will also discuss the advantages, limitations, and prospects for the application of amino acid-based functional systems in the detection of HMs.

1.2. AAs and HMs

The use of AAs for the detection and removal of HMs has attracted significant interest due to their biocompatibility [25] and functional group diversity [1]. The formation of stable complexes with HMs reduces their toxicity and bioavailability. However, their use in HM remediation is poorly studied [1,26]. Examples of AAs studied for the detection and removal of HMs include tyrosine, cysteine, glutamic acid, histidine, etc.

The application of tyrosine is mostly focused on detecting HMs in contaminated environments. Due to the presence of side chains, aromatic phenolic moiety is believed to enhance its ability during binding with metal ions, making it a promising candidate in environmental sensing applications [27]. Hu et al. have proposed four possible interaction modes (Figure 1a–d) of divalent Cu and Zn metal ions with the peptide fragment containing tyrosine in the chelation process. The complex in Figure 1a shows the binding of the metal ion with carbonyl oxygen and nitrogen of the same amide group. This mode of interaction is considered less stable without the interaction of the phenolic group of tyrosine in the resultant complex. Figure 1b–d show the modes of interaction where the aromatic ring in tyrosine is involved in the binding, resulting in more stable complexation due to favorable complex geometries. The aromatic interacts through π interaction to the metal cations and the nitrogen on the adjacent amide group in the coordination. In Figure 1b, the possible interaction of the hydroxy group due to its feasible orientation can also participate, resulting in a more stable interaction. However, in Figure 1c,d, the participation of the hydroxy groups is less likely to be involved in the interaction due to their unfavorable orientation. By looking at the four possible modes, it can be concluded that the metal ion is primarily coordinated by the nitrogen from the amide group and the aromatic ring through π interaction, whereas the participation of the hydroxy group depends on its conformations [1,27].

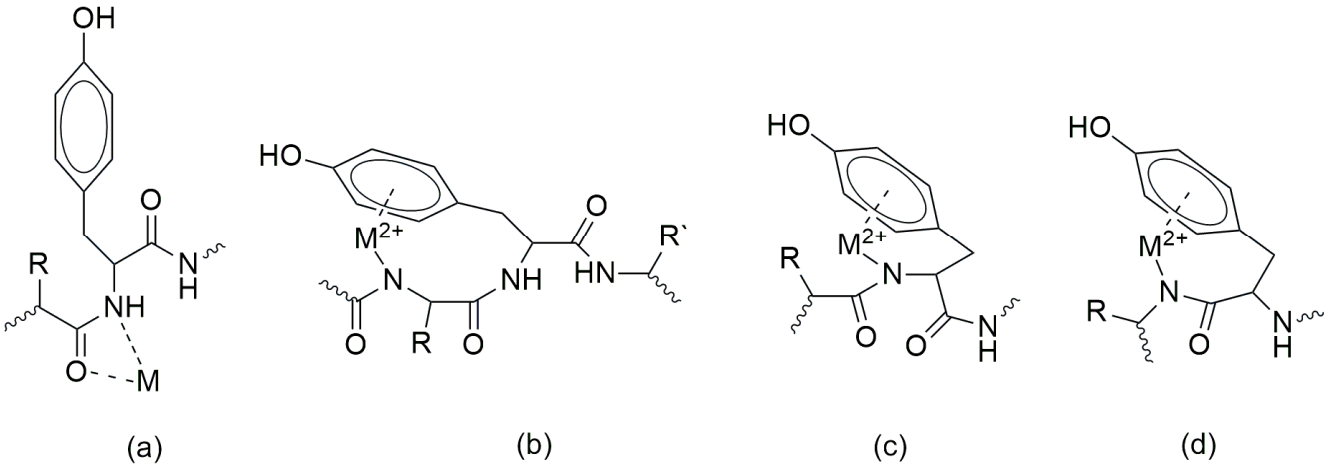


Figure 1. Different possible conformations of the amino acid tyrosine moiety in a peptide with metal ions (**a**–**d**).

Cysteine is another important AA with a thiol side chain, which enables it to form complexes with HMs (Figure 2) [1,28]. The thiol group coordinates with Cd(II) [28], while the thiol and amino groups selectively chelate with Hg(II) ions [29]. Cysteine is a particularly strong ligand for divalent ions such as Cd(II) and Ni(II), because of its good affinity compared to other AAs, and its coordination with metal ions occurs under special conditions where pH > 5.

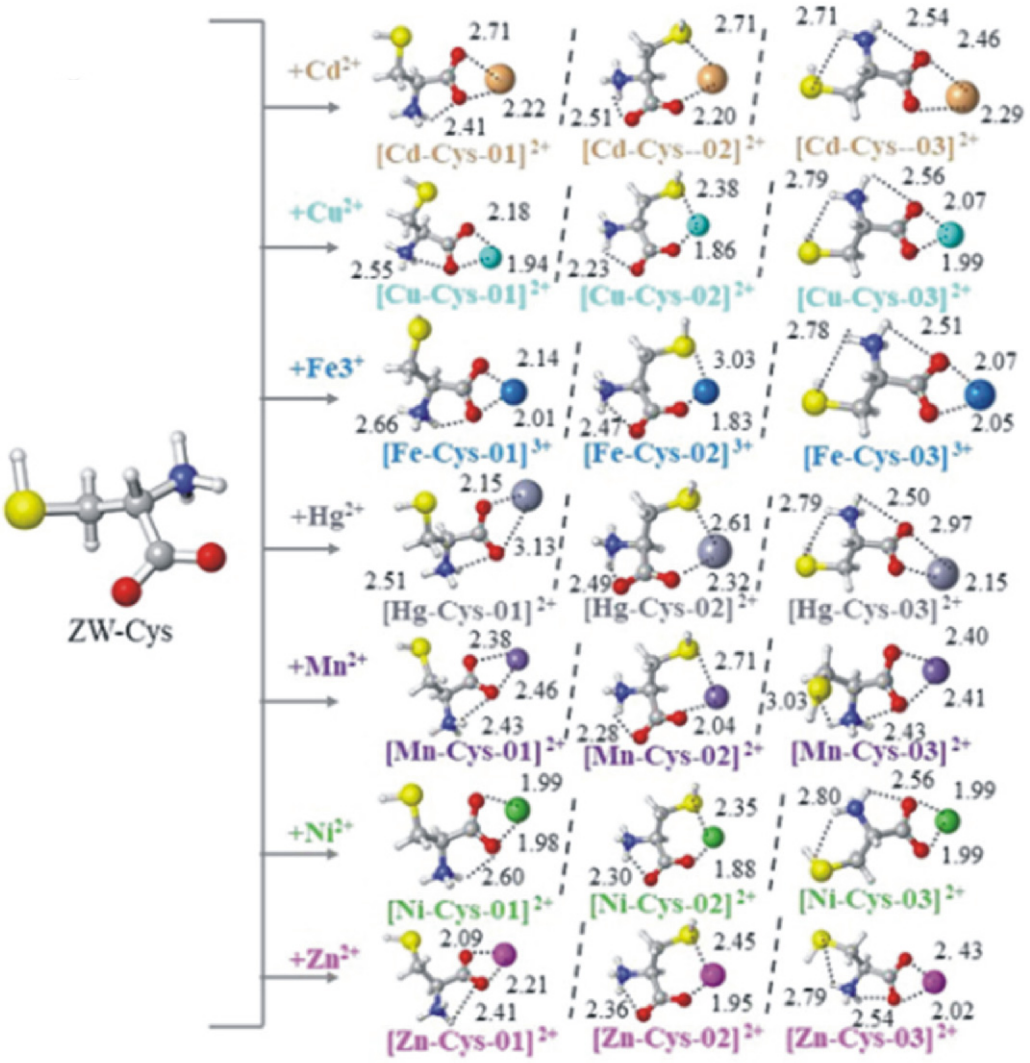


Figure 2. Optimized structure of the cysteine–metal cation complex. Adapted from [3].

Glutamic acid has a carboxylic acid side chain. The interaction with HMs occurs through the β- and γ-carboxylate groups, which act as metal-binding sites (Figure 3). Therefore, glutamic acid acts as a tridentate ligand which forms N-O-O chelates [1]. Many papers have discussed the removal of HMs using poly-γ-glutamic acid, a substance composed of repeating units of *L*-glutamic acid, *D*-glutamic acid, or D*L*-glutamic acid, with an amide bond linking the α-amino and γ-carboxylic acid groups [30–32]. It is a natural synthetic polymer that is biocompatible, water-soluble, biodegradable, and safe to humans. It also exhibits effective removal of Cu, Cd, and Pb ions [30].

Histidine contains an imidazole moiety in its side chain [33]. The imidazole group has a highly polarized, planar, five-membered aromatic ring with amphoteric properties, allowing it to exhibit both acidity and basicity characteristics [1]. The imidazole ring in its side chain readily participates in hydrogen bonding, coordination bonding and cation–π interactions. It also functions as a tridentate by forming a six-membered ring chelating with its carboxylic group [34]. Histidine forms stronger cation–π interactions with Zn(II) than with histidine and Cu(II). However, these interactions reduce the toxicity of Zn and Cu [1,33]. As illustrated in Figure 4, coordination to metal cations like Zn(II) and Cu(II) fundamentally enhances the local chemical reactivity; the metal center strongly polarizes bound water molecules, drastically increasing the interaction energy (ΔE_i) with the solvent.

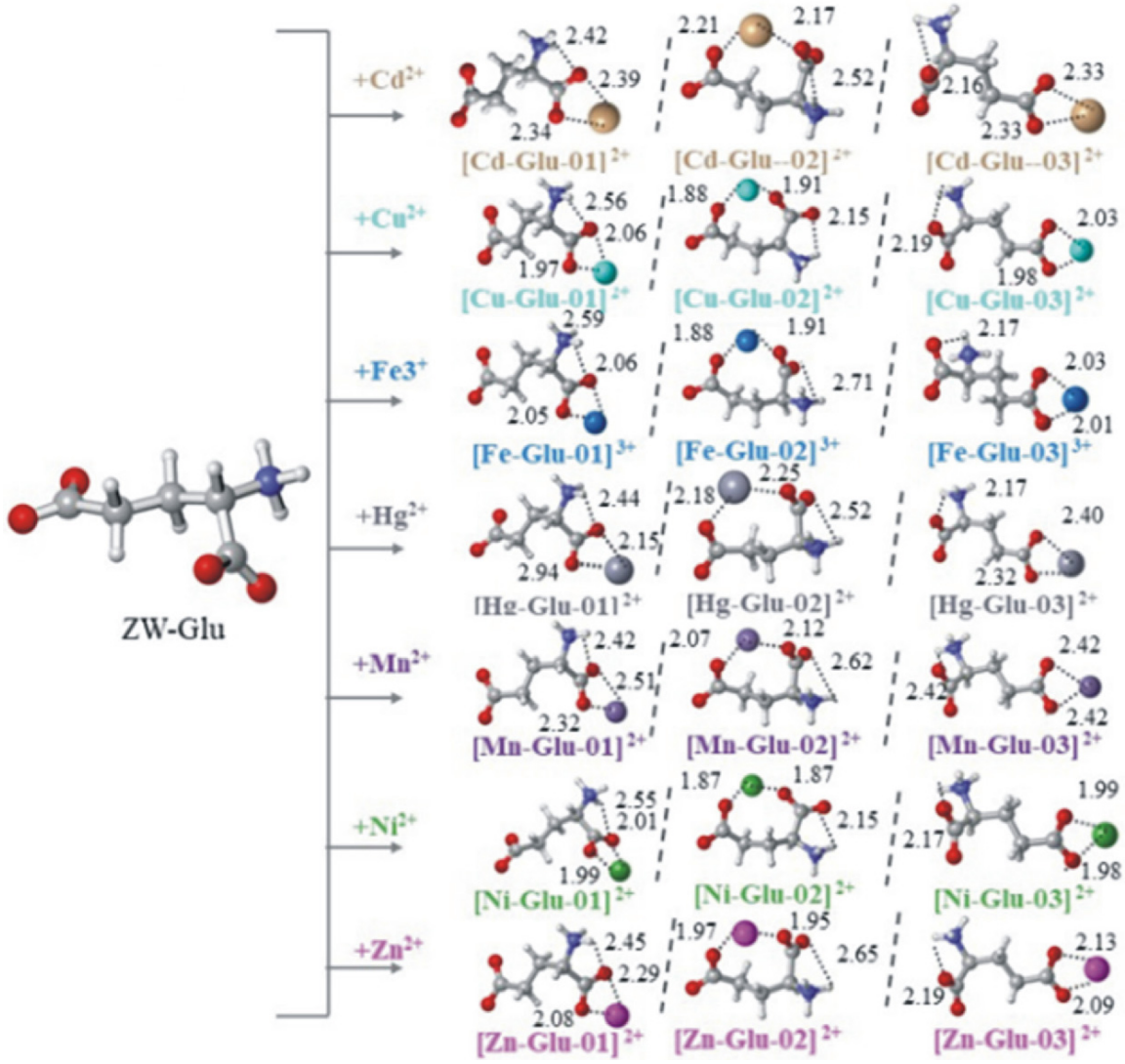


Figure 3. Optimized structure of the glutamic acid–metal cation complex. Adapted from [3].

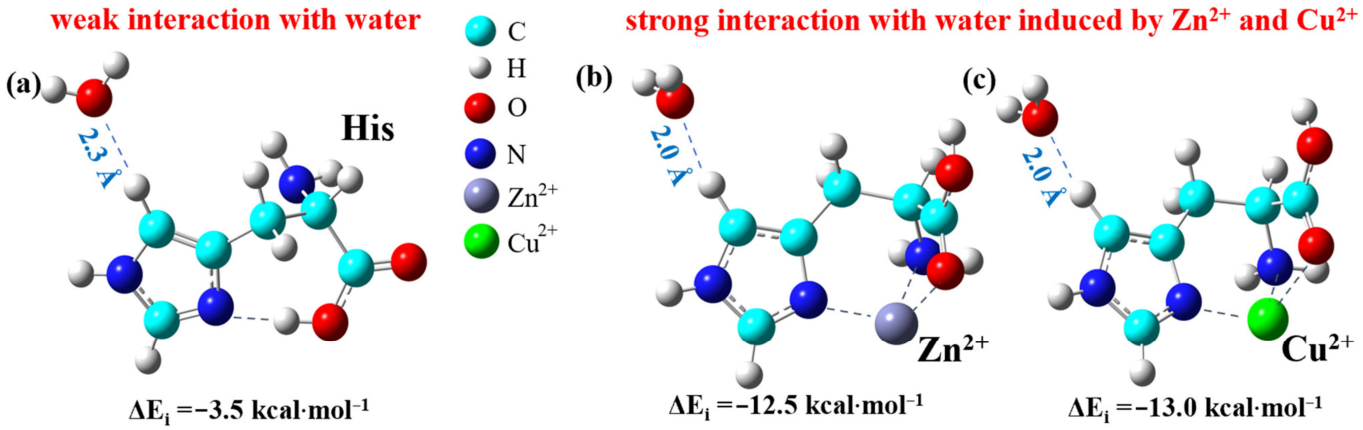


Figure 4. Metal cation enhancement of histidine–water interaction: (**a**) weak interaction of histidine with water; (**b**) strong interaction of histidine with water induced by Zn^{2+}; (**c**) strong interaction of histidine with water induced by Cu^{2+}. Adapted from [33].

1.3. Nanoparticles

The growing need for industrial water recycling has increased research numbers in the nanotechnology field [35]. Research has shown that nanomaterials are effective adsorbents due to their non-toxicity, high adsorption capacity, and recyclability. Additionally, nanomaterials are distinguished by their ease of synthesis and functionality, high active surface area, and chemical flexibility, which increases their use in water treatments. Nanomaterials can be classified into nanoparticles, nanotubes, nanowires, nanosheets, and nanospheres. They are further classified into non-magnetic and magnetic nanomaterials. Magnetic nanoparticles are considered an advanced form of nanomaterials owing to their small size, large surface area, and biocompatibility, which effectively contribute to the removal of HMs from contaminated water. HMs are removed by adsorbing onto the surface of metal nanoparticles (MNPs) [36]. In this context, Au and AgNPs have been explored to a greater extent for the detection of metals. In the following sections, an elaborated description of these nanoparticles is presented.

1.4. Detection Methods of HMs

1.4.1. Electrochemical Methods

These methods are based on electron transfer reactions at an electrode's surface when a suitable potential is applied and a measurable current is produced. Electrochemical methods exhibit very high sensitivity, low cost, are suitable for field detection, need minimal sample preparation and detect a wide range of multiple metals simultaneously. The method uses at least three electrodes: working electrodes where the metal ion reaction occurs, a reference electrode which provides a stable reference potential and a counter electrode which completes the circuit. The anodic stripping voltammetry (ASV) technique is most commonly used for heavy metal detection [37–39]. This technique involves two steps: deposition and stripping. In deposition, a negative potential is applied, and metal ions are reduced and deposited onto the surface of electrode. When potential is directed to a positive potential, deposited metals are oxidized back into solution. Each metal produces a peak current at a characteristic potential, where the peak position identifies the metal, and the peak area measures the concentration.

1.4.2. Optical Detection of Metal Ions

This technique relies on the interactions between metal ions and a detection element, such as a ligand, biomolecule, dye or nanomaterial, which induces a measurable change in the optical signal, such as a change in color, absorbance or emission wavelength, an increase or decrease in fluorescence intensity, or a change in luminescence intensity. This method is characterized by its high sensitivity, cost-effectiveness, speed and suitability for on-site monitoring. Optical detection techniques include colorimetric detection, fluorescence detection, photoluminescent (phosphorescent) detection, surface plasmon resonance (SPR), and localized surface plasma resonance (LSPR), as well as fiber optical sensors.

Colorimetric Detection Technique

This technique relies on the binding of a metal ion, which causes a change in electronic transition and results in a visible color change. While this technique is simple, and the changes can be measured with the naked eyes or using UV-Visible spectroscopy, it is less sensitive than fluorescence methods [40,41].

Fluorescence-Based Detection

This method is based on the binding of the metal ion that causes changes in the intensity of fluorescence. This technique follows several mechanisms, such as photoinduced

electron transfer (PET), chelation-enhanced fluorescence (CHEF), fluorescence resonance energy transfer (FRET) and aggregation-induced emission (AIE). For PET, electrons are transferred from the HOMO of the doped group to the LUMO of the fluorophore [42]. CHEF arises when a fluorophore produces a stable complex with a metal ion, which enhances the intensity of fluorescence [43]. FRET occurs when an excited donor chromophore transfers energy to an acceptor chromophore located at close range [44]. AIE occurs for some molecules the exhibit increased fluorescence when aggregated [45,46].

Luminescent (Phosphorescent) Detection

This technique arises from metal complexes or lanthanides. The limitations of this method are high cost and complexity in synthesis [47].

Surface Plasmon Resonance (SPR) and LSPR

This method relies on the fact that the binding of metal ions causes changes in the refractive index near metallic nanostructures. The detection is typically measured using functionally modified Au nanoparticles. This method is sensitive to environmental changes [48,49].

Optical Fiber and Waveguide Sensors

In this method, functionalized fibers are used and cause a change in transmission or luminescence when metal is bonded [50,51].

2. Gold Nanoparticles (AuNPs)

The biocompatibility, simplicity of surface modification, and quantifiability of gold nanoparticles (AuNPs) have attracted much attention [52]. Gold NPs exhibit interesting size-dependent electronic and optical properties [53]. In addition, they exhibit localized surface plasmon resonance (LSPR), which is generated by interactions between the free electrons and the incident light that result in the red color of the NP solution due to the formation of SPR bands in the spectra region where the color is visible to the naked eye [54]. In the presence of metal ions, the agglomeration with AuNPs causes the solution color to change to blue, resulting in broadening and shifting of the SPR band. This is the reason that AuNPs are widely used in bio- and chemosensors for HM detection [52]. The LSPR characteristics of NPs such as Cu, Ag, and Au greatly increase their effectiveness in colorimetric sensing applications [55].

Simple AuNPs can be used as probes for selective detection of toxic metals in the environment [56]. However, Au nanoparticles produced by chemical reduction are not suitable for functionalization [57]. However, their high surface-to-volume ratio, low dispersion in solution and poor stability and ease aggregation limit their activity and applications [54]; therefore, functionalization of AuNPs is crucial to overcome these limitations.

AuNPs exhibit good interaction capacity with various AAs [57]. AAs are categorized based on their core structure, ionization, side-chain groups, and polarity. These classifications determine their specific binding to AuNP surfaces [58]. AAs can act as reducing agents and capping agents [59]. These capping agents prevent the aggregation of nanoparticles and increase their activity over a long period of time [55]. In addition, AAs, peptides and proteins are environmentally friendly and biocompatible materials that can be used in various applications [60]. AAs are gaining increasing popularity for their ability to produce amino acid-coated AuNPs, thanks to the presence of carboxyl, amine, and thiol functional groups (Figures 5 and 6) [52].

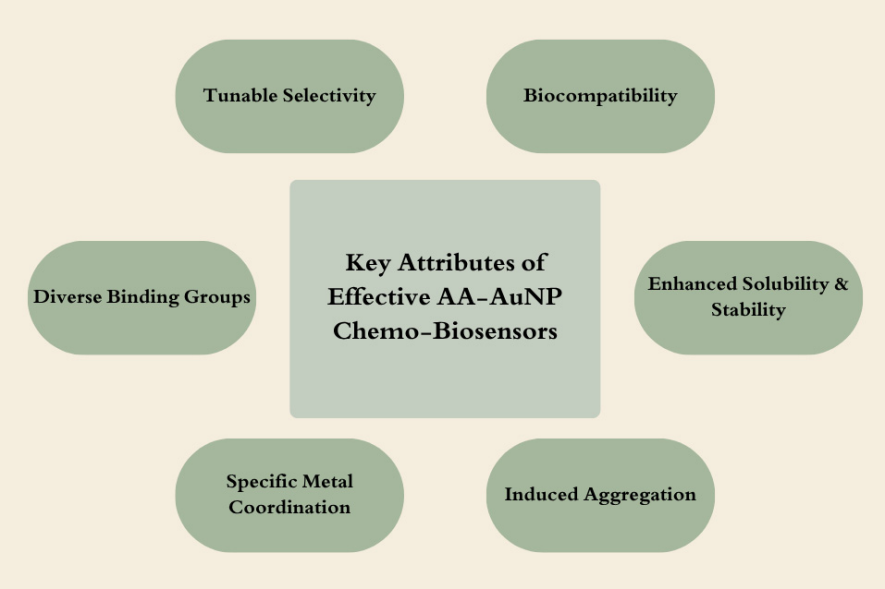


Figure 5. Key attributes of AAs that enable effective AuNP-based chemo-/biosensors.

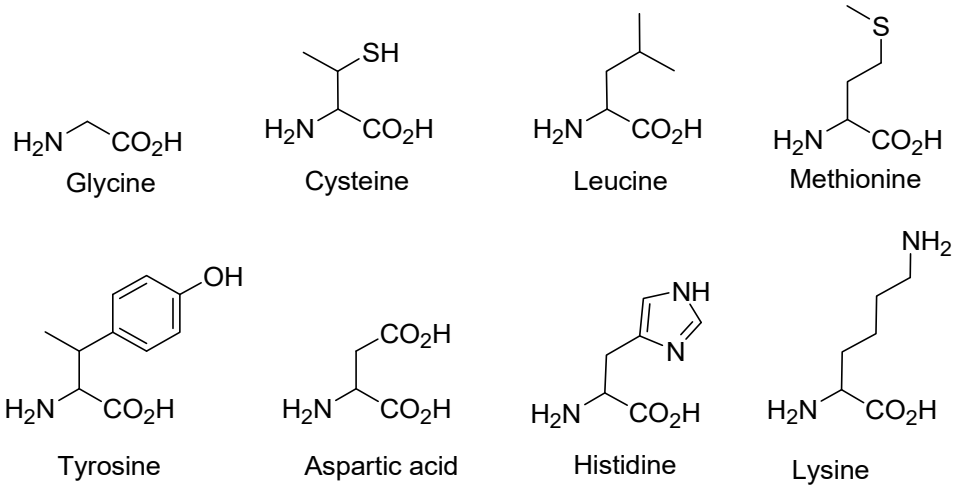


Figure 6. Structures of AAs employed in the functionalization of AuNPs.

2.1. AA-Functionalized AuNPs

2.1.1. Glycine-Functionalized AuNPs

Photochemical synthesis of glycine (Gly)-functionalized AuNPs was performed using a photochemical initiator to study its colorimetric detection of Pb(II) and Hg(II). This study confirms that anionic glycine showed higher affinity for AuNPs, due to its deprotonated amine and carboxylic groups that allow for a strong interaction with the gold surface. On the other hand, neutral and cationic capped AuNPs were unstable and partially larger than the anionic capped AuNPs. Gly-coated AuNPs were used for the colorimetric detection of various metal ions including Ca(II), Mg(II), Cd(II), Co(II), Ni(II), Pb(II), Hg(II), and Zn(II) using the LSPR technique. This study measured the meta-*L*-induced aggregation of Gly-AuNPs, expressed as the ratio of absorbance at 610 nm to 512 nm. The absorption ratio increased with increasing metal ion concentration, indicating NP aggregation. The detection sensitivity varies with different metal ion types. These sensitivities are consistent with the complexation constant of glycine with the corresponding metal ions. Notably, although Hg(II) has the highest complexation constant, the detection sensitivity for Hg^{2+} was not significantly higher than that of Pb(II), indicating differences in binding behavior [61].

Table 1 provides a comparison of anionic, neutral and cationic Gly-AuNPs in terms of stability, size affinity of Gly to AuNPs and sensitivity to detect metal ions.

Table 1. Comparison of Gly-AuNP interactions by metal ions.

Characteristics	Anionic Gly-AuNPs	Neutral/Cationic Gly-AuNPs
Stability	Produced at pH 9 and stable up to one week	Produced at pH 3, sedimentation occurred within a few days after synthesis
Size	5 ± 2 nm	52 ± 17 nm
Affinity of Gly for AuNPs	High adsorption mass density (18 ng/cm^2 at pH 9) Binding energy of anionic glycine with Au clusters (44.0 kcal mol^{-1})	Low adsorption mass density (<2 ng/cm^2 at pH 3) Binding energy of neutral and cationic glycine with Au clusters (15.8 and 7.40 kcal mol^{-1}, respectively)
Detection Sensitivity	Various with different metals	

2.1.2. Cystine-Functionalized AuNPs

L-cysteine (Cys) is effective in stabilizing AuNPs through strong S–Au interactions. Spectroscopic techniques, including UV-Vis, FT-IR, Raman, and NMR, have shown that the presence of Cys in AuNPs helps in the aggregation and enhances their long-term stability through cooperative bonding between ligand donor sites of biomolecules with Au, which in turn provides a larger surface area for the interaction of external analytes [62].

Tables 2 and 3 summarize the key features and findings from four studies conducted on the cysteine-functionalized AuNP surface modified with different ligands, including lipoic acid, 6-mercaptonicotinic acid (MNA), and coumarin, for HM detection (Figure 7). The tables cover the synthesis and detection methods, target HMs, stability, sensitivity, and their applications in real samples. The functional groups of these ligands highlight their potential to provide additional nanoparticle-based chemosensing platforms for environmental and bioanalytical applications with enhanced sensitivity and selectivity, providing an inclusive review of the latest developments in gold nanoparticle technologies.

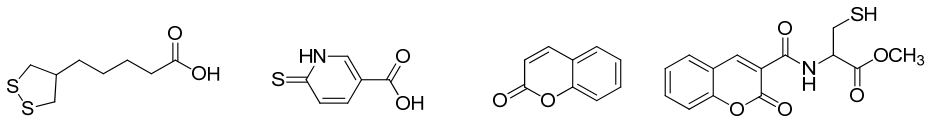


Figure 7. Ligand structures for AuNP functionalization in HM detection: (**a**) lipoic acid; (**b**) 6-mercaptonicotinic acid; (**c**) coumarin; (**d**) an example of coumarin derivative.

2.1.3. Leucine-Functionalized AuNPs

Grosan et al. reported a new approach for improving the electrochemical detection of metal ions (copper), based on AuNPs coated with *L*-leucine or citrate [63]. The idea is to take advantage of nanomaterials, specifically their natural surface area and tunable reactivity, to enhance the sensitivity and specificity of heavy metal ion sensors. The gold substrate was first modified by coating it with a self-assembled monolayer of 1,3-propanedithiol (PDT), and then *L*-leucine-capped AuNPs were attached to the surface, forming a functional surface that interacts with Cu(II) via a chelation process. Using *L*-leucine, this aimed to produce a biocompatible and efficient detector for Cu(II) ions at low concentrations in aqueous solution. This modified electrode showed excellent sensitivity for detecting Cu(II) ions, achieving a limit of detection (LOD) of 5.4×10^{-7} M, making it a highly effective sensing application. The presence of *L*-leucine was shown to allow the chelation of Cu(II)

ions, enhancing the electrochemical response. The electrode was also characterized by using electrochemical impedance spectroscopy (EIS). Since copper ions can create resistance in an electrical circuit, an equivalent circuit was developed to explain the mechanisms occurring at the electrode interface due to their interaction. The changes in charge transfer resistance were observed with increasing copper ion concentration. The performance of a *L*-leucine-capped AuNP electrode was compared with citrate-capped AuNPs and bare gold. The leucine-modified electrode showed superior sensitivity and electrochemical behavior for the detection of Cu(II). This study provides a clear rationale and indicates the importance of altering the electrode surface with functionalized nanoparticles to improve interactions with target analytes, an approach that can certainly be applied in environmental sample analysis and safety monitoring practices.

2.1.4. Methionine-Functionalized AuNPs

In another study, *L*-methionine-AuNPs demonstrated sensitivity and selectivity towards Cr(III) [64]. The LOD for Cr(III) was found to be as low as 300 nM, which was verified by UV-Vis absorption measurements. The absorbance values at 650 nm were quantitatively correlated with Cr(III) concentrations ranging from 0.1 to 5.0 μM. Various metal ions were tested with *L*-methionine-AuNPs, but only Cr(III) significantly altered the optical properties of the AuNPs. This mechanism of sensing is based on metal–ligand interaction. Moreover, other metals in the sample showed no interference with Cr(III) detection.

2.1.5. Tyrosine-Functionalized AuNPs

Tyrosine (Tyr)-functionalized AuNPs were developed as a sensitive colorimetric sensor for the detection of Cr(III) and Pb(II) as stated by [65]. The colorimetric sensing principle illustrates that when Cr(III) or Pb(II) ions are added to a Try-AuNPs solution, a distinct color change is expected. The color shifting from red to blue is a result of the aggregation of AuNPs upon the addition of the metal ions. Moreover, the addition of NaCl induced a rapid color change following the accelerated aggregation facilitated by blocking the repulsion between negatively charged particles. The selectivity of Tyr-AuNPs was evaluated with different metal ions including Fe(II), Zn(II), Cu(II), Cr(VI), and others; however, the aggregation and color shifting were highly observed for Cr(III) and Pb(II). Furthermore, the regeneration and recyclability of Tyr-AuNPs were indicated to be effective for three cycles of Pb(II) and Cr(III) detection. For a period of three months at room temperature, the Tyr-AuNP sensor maintained its integrity and good performance. Therefore, in real water samples the detection of Cr(III) and Pb(II) was highly efficient.

L-tyrosine was previously investigated by Annadhasan et al. as a stabilizing and reducing agent for AuNPs and AgNPs. *L*-Tyr-AuNPs were synthesized in an aqueous medium using a simple and green method [66]. For the detection of Hg(II) and Pb(II), the *L*-Tyr-AuNPs sensor showed a high sensitivity that was attributed to the interactions of the metal ions with the sensor's surface. These interactions result in measurable changes in the SPR band, yielding LODs of 16 nM and 53 nM for Pb(II) and Hg(II), respectively. Moreover, the effectiveness of this sensor in aqueous medium was confirmed by its good stability for 6 months in solution without any noticeable aggregation [66].

2.1.6. Aspartic Acid-Functionalized AuNPs

Wang and co-workers synthesized functionalized AuNPs with aspartic acid using the one-pot method without the need for further modification [67]. Aspartic acid acted as a stabilizing and reducing agent, endowing the nanoparticles with good stability under experimental conditions, as well as excellent optical properties. The Asp-AuNPs were used as a colorimetric sensor for Cr(III) ions based on the dispersion color change, an indicator of agglomeration. The binding occurs between the Cr(III) and the carboxylic groups of

aspartic acid present on the surface of AuNPs [67]. For the detection of Cr(III), the LOD was found to be 0.6 nM, proving the sensitivity of the Asp-AuNPs sensor. Furthermore, the selectivity was assessed with other metal ions and at a concentration five times higher than that of the Cr(III) ions; however, it did not show any interference. Therefore, it was applied to environmental water samples, showing a high recovery percentage reaching 95.4% to 105.1%. Its feasibility for real-world applications was further confirmed by its stability and performance, which were maintained even over eight weeks with minimal changes in its optical properties.

2.1.7. Histidine-Functionalized AuNPs

Histidine was another amino acid investigated as a capping agent for AuNPs. Eviane and co-workers developed AuNPs functionalized with histidine as a colorimetric sensor for the detection of Hg(II) [68]. Optimal conditions for good detection of Hg(II) were observed at a pH of 12 due to the enhanced stability and reactivity of AuNPs, inducing a rapid aggregation and color change from red to black-blue. At that pH, the LOD of Hg(II) reached 1.77 µM, illustrating adequate sensitivity for environmental monitoring. The sensor's sensitivity and selective response to Hg(II) demonstrate its applicability to real-world applications. Therefore, it was successfully applied to industrial wastewater samples and showed high recovery rates, confirming the reliability of the method [68].

Recent research reported a colorimetric and chrominance detection of Zr(IV) using *L*-histidine-AuNPs (*L*-His-AuNPs). Dual-mode detection depends on the interactions between Zr(IV) and the imidazolyl group of histidine. The sensitivity of *L*-His-AuNPs was confirmed with good LOD and linear responses of both colorimetric and chrominance detection. Furthermore, it exhibited high selectivity for Zr(IV) over sixteen other metal ions at the same concentrations. This method is quick, efficient, and cost-effective compared to other traditional methods of detection. In addition, the applicability of this method was proved with 94.90 to 106.05% and 96.51 to 106.54% recovery ranges of colorimetric and chrominance assays, respectively, when applied to natural water samples [69].

2.1.8. Lysine-Functionalized AuNPs

Sener and co-workers developed citrate-capped AuNPs functionalized with lysine for a colorimetric assay of Hg(II) [70]. The assay consists of two steps: First, the interaction between Hg(II) ions with the surface of AuNPs forms a mercury layer due to the spontaneous deposition on the surface. Second, lysine with its amino group is responsible for catalyzing the aggregation of AuNPs bearing Hg(II) by facilitating the formation of bridges between the AuNPs. Therefore, a rapid color shift from red to purple or gray occurs in a few seconds upon addition of lysine to the solution. However, this aggregation and the rapid change in color were noticed only with Hg(II) compared to other metal ions. Moreover, this method proved its effectiveness when applied to distilled water and tap water samples, by detecting all the spiked concentration with high accuracy. The recovery rates of this method almost reached 100%, demonstrating its reliability and practicality. Furthermore, the low cost of this assay broadens its range of applications in environmental monitoring and freshwater resource assessment. The applicability of this method in field and laboratory settings is facilitated by easy color visualization or measurement of color response using a UV-Vis spectrophotometer.

2.1.9. AA Crosslinking for Enhanced Sensitivity

Metal ions including Cu(II) and Pb(II) were simultaneously detected using an electrochemical microsensor developed through a micro-electro-mechanical system technique. One of the sensor design's major innovations was the production of a crosslinked amino acid layer. This was done by initially mounting *L-cysteine* on the AuNP-coated surface

and subsequently binding *L*-aspartic acid to it with glutaraldehyde as a crosslinker. The intended crosslinking approach was critical, as it formed a thick, stable monolayer with a greatly increased number of carboxyl groups for metal-ion complexation compared with a single amino acid layer. The sensor's sensitivity was confirmed by its excellent linear range and low detection limits for Cu(II) and Pb(II). Furthermore, the sensor showed excellent stability and could be regenerated with acetic acid without significant loss of function, maintaining an efficiency of around 80% after multiple uses [71].

2.1.10. AA Bifunctionalization of AuNPs

A novel approach for the detection of Cu(II) and Hg(II) using methionine- and cysteine-functionalized AuNPs and stabilized with polyvinylpyrrolidone (PVP) demonstrated strong anti-interference from different ions and organic compounds, making them suitable for complex biological fluids such as urine and serum. The binding between the modified AuNPs and Cu(II) and Hg(II) leads to crosslinking aggregation of the AuNPs, thus resulting in a visual color change. Absorbance ratios can be measured via UV-Vis spectroscopy to quantify these colorimetric changes. The different sensors exhibit LODs of 2.34 μM for Cu(II) and 0.026 μM for Hg(II), with concentration ranges of 3.0–500.0 μM and 0.5–500.0 μM, respectively. The sensor showed good recovery rates that matched scientific studies and validated test results on actual samples (including human urine and serum), indicating the feasibility of these sensors for monitoring HMs in biological fluids (among other complex matrices). Recovery rates for spiked samples of Cu(II) ranged from 93.20% to 108.10%, while the recovery range for Hg(II) ranged from 95.60% to 106.80%, which are acceptable reference ranges of accuracy and reliability. Since PVP provides stabilizing properties to AuNPs, the stability of PVP-AuNPs was tested at different pH levels (2.0–12.0), as well as whether it reaches stability based on temperature conditions. It had proven effective in preventing aggregate formation when combined with PVP [72].

2.1.11. Peptide-Functionalized AuNPs

Capping agents act as a key factor in determining the structure, shape, size, and properties of nanoparticles, making them vital for desired applications. Traditionally, the ligand exchanging process that is used to modify nanoparticle surfaces is a relatively lengthy process, which can result in partial coatings or contamination [73]. Therefore, it is advantageous to synthesize nanoparticles with a capping agent. Also, if the capping agent can reduce metal ions, adding additional reducing agents becomes unnecessary. Given that most nanoparticle synthesis methods require specialized conditions, it is necessary to identify methods that enable synthesis at room temperature [74]. The stabilization of nanoparticles can be obtained using peptides as ligands, posing a distinct design versatility. AAs, or existing amino acid residues, can be manipulated to design multifunctional peptides that not only stabilize nanoparticles but also carry functions of molecular recognition, catalysis, drug delivery, and sensing [75–78]. Additionally, the formation of core/shell nanoparticles and the detection of various metal ions can be achieved using peptides [74]. Molecular dynamics studies reveal diverse interactions and how AAs and sequences influence binding affinity [79]. The peptide's binding affinity to gold surfaces depends on the amino acid sequence, with aromatic rings (tyrosine, phenylalanine) and cysteine residues serving as potent docking sites [80,81]. The sizes of AuNPs also affect binding properties, with smaller NPs being able to produce higher binding selectivity by attracting highly reactive AAs. Moreover, peptide binding also regulates amyloidogenic peptide fibrillation [82].

Peptides reduce and cap AuNPs, tuning their size and morphology. The demonstration of certain AAs in the sequence, such as tryptophan and others, can accelerate the reduction

in Au ions. At the same time, cysteine-bearing peptides reduce the rate of synthesis of AuNPs by binding to gold cores, thus a inhibiting further reduction in gold ions. Therefore, controlling the formation and growth kinetics, and consequently the shape, size, and uniformity of Au, should be achieved by adjusting the peptide's isoelectric point (pI) and the peptide-to-gold-ion ratio in the reaction solution. According to density functional theory calculations, cysteine, aspartic acid, and tryptophan provide the highest adsorption affinity for Au surfaces [52].

2.1.12. Dipeptide-Functionalized AuNPs

Functionalized dipeptide AuNPs are promising candidates for the precise detection of HMs due to their distinct optical and electronic properties. Glycine–histidine dipeptides (Figure 8) are examples of dipeptides that enable precise functionalization of AuNPs, thereby increasing their interaction with metal ions by providing specific binding sites. A colorimetric determination assay of Cu(II) NPs using Gly/His-AuNPs showed that the modifications indeed change the optical properties of the NPs due to a redshift in the absorption spectrum upon interaction with the metal ions. Moreover, greater selectivity for Cu(II) was confirmed through a comparison with other metal ions, signifying their effectiveness in complex matrices such as tap water. The application of this method for tap water samples showed a recovery range between 102% and 104%. This study reported the potential of using dipeptide molecules to detect other toxic species [83].

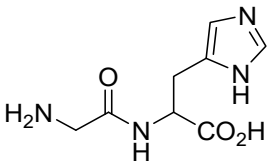


Figure 8. Structure of glycine–histidine dipeptide.

Gunupuru developed a dipeptide-functionalized AuNP sensor for the detection of Cr(III), Pb(II), and Hg(II) [84]. The glycylglycine (GG) dipeptide consists of two glycine molecules that enhance the interaction between the metal ions and their amine and carboxyl groups (Figure 9). Through these interactions, the GG-AuNPs aggregate via inter-particle plasmon coupling and exhibit significant color changes from dark red to gray blue. The detection limits were 1.0 μM for Cr(III), 2.5 μM for Pb(II), and 3.0 μM for Hg(II), indicating the efficiency of colorimetric detection. Overall, this sensor showed great accuracy in the detection of Cr(III), Pb(II), and Hg(II), with insignificant interference from other metal ions [84].

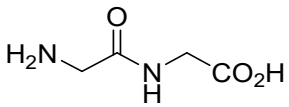


Figure 9. Structure of glycylglycine (GG).

2.1.13. Tripeptide-Functionalized AuNPs

A naturally occurring tripeptide, glutathione (GSH), possesses an exceptional structural characteristic including numerous coordination sites and a reduced thiol moiety (Figure 10). These characteristics contribute to its physiological importance and ability to act as a ligand for the enhancement of metallic NPs [85]. Moreover, the functionalization of magnetic, fluorescent metallic, and hybrid types of NPs with GSH enhances their colloidal stability and biocompatibility for biomedical and sensing applications. Although it is in principle non-toxic, the degree of passivation of toxicity depends on the nanoparticle's core material. The following studies have collectively demonstrated the contribution of

glutathione to the development of sensitive, selective, and practical heavy metal detection systems [86].

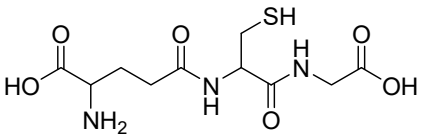


Figure 10. Structure of glutathione (GSH).

GSH is applied in heavy metal detection. Its main function is to chelate nanoparticles, especially gold nanoparticles [87]. The crucial factor is the carboxyl functional groups within GSH, which directly coordinate with HM ions such as lead (Pb(II)). This chelation leads to the agglomeration and self-assembly of GSH-functionalized AuNPs. The degree of aggregation depends on the concentration of HM ions. The aggregation affects plasmonic coupling, thereby shifting the plasmon wavelength. For example, when detecting Pb(II), the shift causes an obvious color change, allowing for rapid and easy colorimetric or optical detection of the metal [87].

In addition to its optical detection, the special chemical structure of glutathione, with its -SH, -COOH, and -NH_2 groups, enables its use for the selective capture of HM ions in electrochemical sensing. When adsorbed onto AuNPs and multi-walled carbon nanotubes (thus MWCNTs-GSH-Au-GSH), glutathione also provides a sensitive and interference-resistant sensing interface. The composite material combines the heavy metal capture properties with the electrocatalytic characteristics of gold nanoparticles, resulting in a highly sensitive system capable of detecting HMs, even at very low concentrations, such as Pb(II) in complex samples such as rice phloem sap [88].

2.1.14. Protein-Functionalized AuNPs

Guo et al. described a rapid and economical colorimetric technique for the simultaneous detection of Pb(II), Hg(II), and Cu(II) ions, exploiting papain functionalized AuNPs (P-AuNPs). Papain, a protein containing many cysteine residues, selectively binds to these metal ions, causing the color of the NP solution to change from red to blue as a result of aggregation. The detection method was quite sensitive, up to a maximum of 200 nM per ion, with Hg(II) exhibiting the strongest colorimetric response. However, the solution pH, in addition to the concentration and the size of the P-AuNPs, influences its sensitivity. It was demonstrated that better results were obtained from the larger AuNPs. This colorimetric method was applied to real water samples without requiring any cleanup or pretreatment methods. Overall, P-AuNPs appear to provide a viable method for detecting toxic HMs in aquatic environments [89].

Table 2. Functionalized AuNPs for heavy metal detection using colorimetric method of detection.

Functionalizing Agents	Targeted Metals and Sensitivity	Real Sample Application	Stability and Reusability
Glycine [61]	LOD: 5 µM for Hg(II), Pb(II), Cd(II)15 µM for Ni(II), Zn(II), Co(II); and >20 µM for Mg(II) and Ca(II)	Not specified	Stable for up to 3 months
L-cysteine [90]	LOD: 290 ppb for Pb(II) and 140.35 ppb for Hg(II)	Effective in a real water sample	Stable at pH 6.2 and 7.0; unstable at pH 9.0; consistent absorbance over 5 days, allowing detection without interference
L-cysteine [91]	Detectable concentrations up to 40 ppm for Cd(II)	Applied to milk samples	Stable at room temperature

Table 2. *Cont.*

Functionalizing Agents	Targeted Metals and Sensitivity	Real Sample Application	Stability and Reusability
Tyrosine [65]	LOD: 1 μM for Cr(III); 2 μM for Pb(II)	Applied to drinking water, seawater, and lake water samples	Stable for 3 months at room temperature; good recyclability demonstrated
Tyrosine [66]	LOD: 16 nM for Pb(II); 53 nM for Hg(II)	Applied to drinking water and tap water samples	Stable for up to six months
Aspartic acid [67]	LOD: 0.6 nM for Cr(III)	Applied to environmental water samples	Retains stability for eight weeks at 4 °C without significant performance degradation
L-Histidine [68]	LOD: 1.77 μM for Hg(II)	Applied to industrial wastewater samples	Stable in alkaline conditions
Lysine [70]	LOD: 2.9 nM for Hg(II)	Applied for distilled and tap water	-
Methionine/cysteine/PVP modified [72]	LOD: 2.34 μM for Cu(II) and 0.026 μM for Hg(II)	Potential application in tab water, urine, and serum biological fluids.	High stability under temperature fluctuations and pH changes
Glycine–histidine dipeptide [83]	LOD: 0.08 mgL^{-1} for Cu(II)	Applied to tap water	Not specified
Glycylglycine [84]	LOD: 1.0 μM for Cr(III), 2.5 μM for Pb(II), and 3.0 μM for Hg(II)	Potential application in water	Highly stable
Papain [89]	Detect Hg(II), Pb(II), Cu(II) at concentration as low as 200 nM	Applied for real water samples	Stable at high pH

Table 3. Functionalized AuNPs for heavy metal detection using various detection methods.

Functionalizing Agents	Detection Method	Targeted Metals and Sensitivity	Real Sample Application	Stability and Reusability
L-cysteine/Lipoic acid [92]	Square-wave anodic stripping voltammetry (SWV-ASV)	LOD: 3 ppb; dynamic range: 3–25 ppb for As(III)	Applied to groundwater samples	Stable at 4 °C for up to 30 days
L-cysteine/MNA [93]	Theoretical (DFT-D3)	Highest sensitivity with MNA-CYS-AuNPs; strong electrostatic interactions for Cd(III)	Theoretical validation	-
L-cysteine/Coumarin AuNPs [94]	UV-Vis absorption and fluorescence spectroscopy	Strong complexation with Zn(II), Cd(II), and Ag(I); L1 shows higher sensitivity	Not specified	Stable in solution for 4 months; no significant aggregation observed
L-cysteine/Electrodeposition on ITO glass [95]	SWV and LSPR	LOD: <5 nM (0.31 ppb); linear range: 10–100,000 nM for Cu(II)	Applied to tap water samples	High stability
L-Leucine/Modified electrode [63]	Cyclic voltammetry (CV)	LOD: 5.4×10^{-7} M for Cu(II)	-	-
L-Methionine [64]	Colorimetric (UV-Vis absorption and surface-enhanced Raman scattering (SERS))	LOD: 300 nM for Cr(III)	Applied to tap water, river water, and seawater samples	Stable
L-Histidine [69]	Colorimetric, and chrominance	Colorimetric LOD: 2.62 μmol L^{-1} for Zr(IV) Chrominance LOD: 6.25 μmol L^{-1} for Zr(IV)	Applied to tap and river water samples, and sewage from treatment plants	Stability obtained at 4 °C and maintained for up to 10 days.
L-aspartic acid/*L-cysteine* [71]	Electrochemical, SWV	LOD: 1 μg L^{-1} for Cu(II) and Pb(II)	Potential application in HMs analysis	For up to 20 days, the current response retained 89.2% for Cu(II) and 86.3% for Pb(II) of the original response
Glutathione/multi-walled carbon nanotubes [88]	Electrochemical	LOD: 0.01 μM for Pb(II)	Applied in rich phloem sap	Excellent stability for over 6 months

3. Silver Nanoparticles (AgNPs)

Nanomaterial diameters range from 1 to 100 nm; in this range, the chemical, physical, and biological properties of noble metals vary significantly from those of their bulk form, because of their small particle size, high surface area-to-volume ratio, and quantum confinement effects [96]. The shape, size, and size distribution of metal NPs are the properties that govern their electromagnetic, optical, electrical, and catalytic properties. These parameters can be influenced by the choice of synthetic method, reducing agent, and stabilizer. As a result of their small size, NPs have a very high surface area compared to their volume; thus, they have great antibacterial activity that is not observed in bulk silver. The reason is that the increased surface area is more reactive; consequently, there are more effective interactions with microbial cells [97].

AgNPs gained great consideration due to their usefulness in diverse fields (Figure 11). They are widely used in medicine and healthcare as fine antimicrobial agents, effective against a wide spectrum of bacteria, including multidrug-resistant strains. Their antibacterial capabilities stem from multiple mechanisms of action, allowing them to simultaneously attack microorganisms in different ways [98]. Furthermore, they have been employed in food packaging to prevent contamination and in catalyzing various industrial processes due to their excellent conductivity and chemical stability. Manipulating size and shape can assist in drug target identification, diagnosis, detection, and imaging [97].

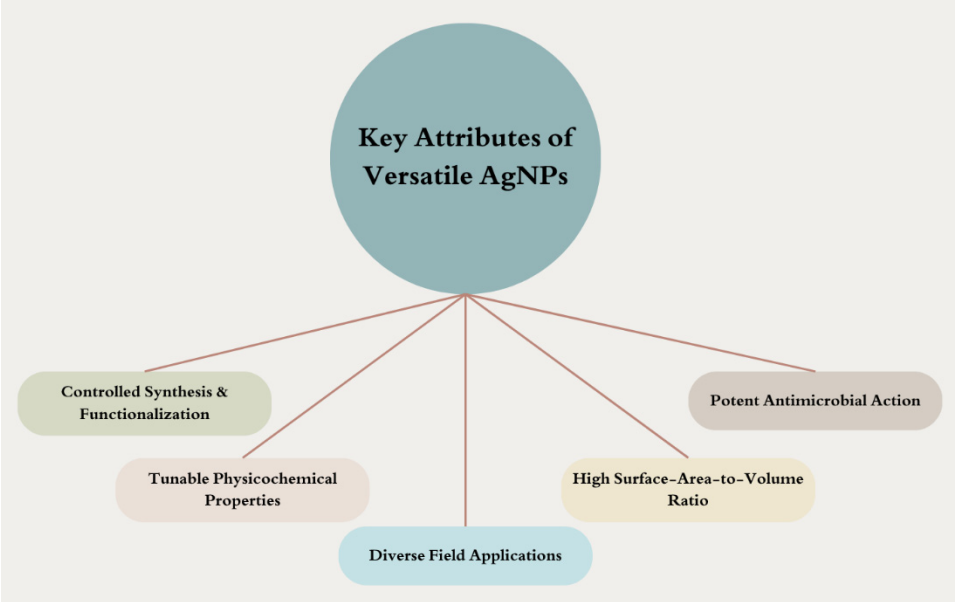


Figure 11. Key functional attributes of silver nanoparticles (AgNPs).

Stabilizing or capping agents control the morphology of AgNPs, prevent aggregation, and control its unique properties. The electromagnetic, optical, electrical, and catalytic properties are controlled by the shape, size, and functionalized AgNP distribution [96,97].

3.1. Amino Acid-Functionalized AgNPs

3.1.1. Glycine-Functionalized AgNPs

Janani et al. developed starch-stabilized AgNPs conjugated with glycine as a colorimetric sensor for the rapid detection of Hg(II) (Table 4) [98]. Synthesis of this sensor included the chemical reduction method for capping the starch and stabilizing the AgNPs. Then, the conjugate formation with glycine facilitates the interactions with Hg(II). These interactions allowed colorimetric detection by causing the color to change from yellow to colorless. An inverse relationship between the concentration of Hg(II) and the intensity of

the UV-Vis absorption band was observed. Therefore, the LOD was very low at 17 nM for Hg(II) compared with other detection methods. This method can potentially be applied at nanomolar levels with high selectivity for Hg(II) and insignificant interference. Furthermore, the sensor's sensing potential remained unaffected for over a month. Hence, it was successfully used for the analysis of Hg(II) in Bhavani River water (74 nM), and the results were validated by atomic absorption spectroscopy [98]. Burrati and co-workers inserted AgNPs capped with citrate and *L*-cysteine into poly(ethylene glycol) diacrylate hydrogels and applied successfully for the removal of Hg(II) ions from water samples [99].

Table 4. Functionalized AgNPs for heavy metal detection and removal.

Functionalizing Agents	Detection Method	Targeted Metals and Sensitivity	Real Sample Application	Stability/Regeneration and Reusability
Glycine/starch modified [98]	Colorimetric	LOD: 17 nM for Hg(II)	Applied to samples collected from the Bhavani River	After a month of retention, they sustained excellent selectivity
L-cysteine/citrate inserted into poly(ethylene glycol) diacrylate hydrogels [99]	Chemisorption	Removal efficiency of 94% for Hg(II)	Applied to 10 mL of Hg(II) polluted water at 8 mg/L	-
Glycine-modified chitosan [100]	Adsorption via ion exchange	Loading capacity: 270.2 mg/g removal efficiency of 93% for Pb(II)	-	Regeneration by acid treatments. The removal efficiency declines after the first two cycles.
L-cysteine/trisodium citrate [101]	Adsorption	Maximum lead adsorption capacity of 105.4 mg/g for Pb(II)	-	-
L-cysteine [102]	Colorimetric	LOD: 45.39 nM for Hg(II) and 49.39 nM for Pb(II)	Applied to tab water samples	Highly stable, stored at 5 °C
Methionine [103]	Colorimetric	Sensitive, sensitivity decreases with an increase in concentration of Hg(II)	Applied to sewage water treatment plants	-
Tyrosine [104]	Fluorescence	LOD: 36 ppb for Cu(II) and 48 ppb for Co(II)	-	Stable for several weeks
Histidine [105]	-	-	-	Stability obtained at room temperature and maintained for up to one month
Arginine/loaded graphene hydrogel [106]	Adsorption	Maximum adsorption capacity is 434.78 mg/g for U(VI)	Applied to simulated seawater	The desorption efficiency was 91.6% for the first time. The desorption efficiency still reached 80.21% after the fifth cycle.
Glutamine/histidine [107]	Colorimetric	LOD: 25.48 μM for Hg(II)	Applied to real water samples (drinking water, tap water, and river water)	Stable for over 1 to 17 days at room temperature

Recent research has developed a green approach to incorporating AgNPs into glycine-modified chitosan (SCG) for the adsorption of Pb(II). The binding affinity of SCG-AgNPs for HM ions was provided through the amino and hydroxyl groups in chitosan polymers. The strong interaction with these groups adsorbs Pb(II) via ion exchange, adsorption, and electrostatic attraction. The significant increase and improvement in adsorption are attributable to the glycine modification. The effectiveness of the ion exchange mechanism was confirmed by the Langmuir isotherm and pseudo-second-order kinetic models. Moreover, ion exchange plays an important role in the mechanism supported by an average potential energy of 9.4 kJ/mol. The study reports that the glycine-modified chitosan-stabilized AgNPs demonstrated an improved loading capacity of Pb(II) of 270.2 mg/g with a removal

efficiency of 93% from aqueous solution. The removal efficiency of SCG-AgNPs was preserved even after multiple cycles. Therefore, these modified AgNPs have great potential for practical applications in environmental remediation. In addition, it exhibited good antioxidant activity and wide antibacterial activity [100].

3.1.2. Cysteine-Functionalized AgNPs

Hosseini et al. investigated an environmentally friendly and effective approach to synthesizing surface-modified AgNPs for the removal of Pb(II) [101]. *L-cysteine* was used as a functionalizing agent and trisodium citrate as a reducing agent. Parameters, including the amounts of precursors and agents, were controlled by response surface methodology (RSM). These parameters affect the synthesis of AgNPs and their effectiveness in removing Pb(II) ions. According to the analysis of variance (ANOVA), the sodium citrate concentration had the greatest influence on lead removal efficiency. The effective removal of Pb(II) from contaminated water was maintained at a maximum adsorption capacity of 105.4 mg/g. Furthermore, the highest adsorption was observed at slightly acidic conditions. Overall, this method outperformed other reported methods in both adsorption capacity and contact time, highlighting the efficiency of lead removal from water using *L-cysteine*-AgNPs [101].

Recent research investigating cysteine as a capping agent for enhanced properties of AgNPs and application in HM identification synthesized Cys-AgNPs as a dual-color sensor for the detection of Hg(II) and Pb(II) in water. The functionalization of AgNPs with cysteine and their stability were confirmed through various characterization techniques such as UV-Vis spectroscopy, SEM, and FTIR. Upon the interaction of Hg(II) and Pb(II) with Cys-AgNPs, the color changed from yellow to white and dark yellow, respectively. The color changing from yellow to orange during simultaneous detection indicated the successful chelation and aggregation of HMs with the nanoparticles. LOD was 45.39 nM for Hg(II) and 49.39 nM for Pb(II). These values demonstrate high sensitivity for both ions. The study confirmed that Cys-AgNPs selectively detected Hg(II) and Pb(II) over other metal ions, demonstrating their suitability for real-world water sample applications. Experiments were also conducted on real water samples and found Cys-AgNPs to be effective and reliable in identifying HM contamination [101].

3.1.3. Methionine-Functionalized AgNPs

Balasurya and co-workers reported that a AgNP-based sensor was established for the rapid and highly sensitive colorimetric identification of Hg(II) ions at nanomolar levels [103]. The synthesized AgNPs were stabilized by PVP and conjugated to methionine. Hg(II) detection in a system using AgNPs depends on the aggregation of NPs in the presence of Hg(II) ions. One reason for this strong aggregation is the strong affinity between Hg(II) and sulfur in methionine. The addition of Hg(II) to the AgNPs–methionine conjugate can induce electron transfer via a redox mechanism, leading to changes in particle size and zeta potential. The appearance of a color change from yellow brown to colorless indicates the presence of the Hg(II) ions. The sensor showed high sensitivity and selectivity for Hg(II), with linear detection ranges of 20–100 nM and no interference from other metals. Moreover, the effect of pH, temperature, salinity, on the detection efficiency of the sensor was investigated. A good detection efficiency was obtained at an optimal temperature of 35 °C, where good binding and sensitivity were observed. In addition, efficiency was affected by the decrease in pH, and its highest point was reached at pH 8. However, the sensor remained stable across different salinity levels. Furthermore, Balasurya and co-workers discussed the potential application of AgNPs–methionine sensor in real water samples for environmental monitoring [103].

3.1.4. Tyrosine-Functionalized AgNPs

Contino and co-workers explored a fluorescence sensor of *L*-tyrosine functionalized AgNPs for the detection of Cu(II) and Co(II) ions [104]. Synthesis of AgNPs was performed following the method pioneered by Creighton in 1979 with slight enhancement of the procedure. In addition, UV-Vis spectroscopy, transmission electron microscopy (TEM) and dynamic light scattering (DLS) were used to characterize AgNPs, indicating their stable colloidal behavior for up to a month. Moreover, UV-Vis demonstrated a linear relationship between metal ion concentration and the decrease in silver surface plasmon adsorption and indicated effective coordination with surface-attached tyrosine groups. Fluorescence experiments showed extremely high fluorescence intensity for the *L*-Tyr-capped AgNPs, which was quenched upon addition of metal ions. Stern–Volmer plots confirmed the linear relation of fluorescence quenching against metal ion concentration, with detection limits of 36 ppb for Cu(II) and 48 ppb for Co(II). Overall, the study demonstrated *L*-tyrosine-capped AgNPs as a facile, sensitive, and rapid method for the detection of heavy metal ions in aqueous solutions [104].

3.1.5. Histidine-Functionalized AgNPs

Liu et al. presented the synthesis and characterization of *L*-histidine (His)-capped AgNPs using a hydrothermal method to obtain a stable and biocompatible nanoparticle system for sensing purposes, focusing on the detection of Ni(II) in aqueous solutions [105]. The His-AgNPs were characterized by TEM and atomic force microscopy (AFM), with an average diameter and height of 21 ± 2 nm and 21 ± 3 nm, respectively. The zeta potential of -24.25 ± 1.10 mV measured by DLS indicated their good stability in solution. Moreover, SERS results showed that the imidazole group of histidine is bound to the Ag surface, while the COO^- group remains exposed to interact with analytes. Upon addition of nickel chloride ($NiCl_2$), the color of the colloidal silver solution changed from yellow to reddish-brown, and a shift in SPR peak was also observed, suggesting the aggregation of the nanoparticles and the detectability of nickel ions. Furthermore, the synthesized His-AgNPs showed remarkable stability in aqueous solutions, maintaining their efficiency for about one month, which is essential for any real-world applications in sensing and biomedicine [105].

3.1.6. Arginine-Functionalized AgNPs

Zhu and co-workers developed an adsorbent of *L*-arginine–graphene hydrogel loaded with AgNPs (Ag-*L*-Arg-rGH) for U(VI) from seawater. The synthesis of Ag-*L*-Arg-rGH composites was performed in a one-step thermal reduction process. The role of *L*-arginine (Figure 12) is that of a functionalizing and crosslinking agent. These composites exhibited a maximum U(VI) adsorption capacity of 434.78 mg/g, according to the Langmuir isotherm model, proposing the monolayer adsorption on a homogeneous surface. The adsorption kinetics showed good correlation with the pseudo-second-order model, indicating that chemical adsorption is the rate-controlling step. A high selectivity of Ag-*L*-Arg-rGH composite was observed in the presence of competing metal ions with a distribution coefficient (Kd) value of 2.41×10^4 mL/g. Additionally, it exhibited anti-algae effects and a reduction in algal growth during the soaking experiments. Its good performance was monitored in simulated sweater systems, indicating the high removal rates of uranium and the promising practical applications in osteointegration of uranium from natural seawater. Moreover, this good performance was retained even after several adsorption–desorption cycles, highlighting that it can be reused in real-world applications [106].

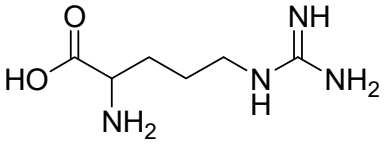


Figure 12. Structure of *L*-arginine.

3.1.7. AA Bifunctionalization of AgNPs

For the detection of Hg(II) ions, a simple and rapid detection sensor based on glutamine- and histidine-functionalized AgNPs (Gln-His-AgNPs) was developed by Buduru et al. The synthesis of AgNPs included the reduction in $AgNO_3$ with $NaBH_4$ where Gln and His were acting as capping agents. Characterization techniques of UV-Vis, FT-IR, and TEM confirmed the successful functionalization process of stable NPs having 10 nm diameter. Upon the addition of Hg(II) ions, the aggregation of Gln-His-AgNPs occurs and results in the color change from yellow to orange. The coordinate covalent bonding between Hg(II) and the functional groups of Gln and His on the surface of AgNPs causes a red shift in the SPR peak from 407 nm to 480 nm. The linear response of the method ranges from 100 to 1000 µM of Hg(II), with an LOD of 0.90 µM. The presence of 0.2 M NaCl enhanced sensitivity, promoting aggregation without interference. Gln-His-AgNPs showed excellent selectivity for Hg(II) in the presence of other metal ions, because Hg(II) alone causes significant changes in the UV-Vis spectrum and color of the NPs. This method has been effectively applied to Hg(II) detection in real water samples (drinking, tap, and river water) with a range of recovery rates of 95.00 to 98.66% [107].

4. Bimetallic Nanoparticles (BNPs)

Bimetallic nanoparticles (BNPs) are a unique class of nanomaterials, synthesized by mixing two metallic components. These fine nanostructures offer superior properties compared to their monometallic counterparts, making them of great interest for scientific and technological applications. The way BNPs organize the two metals and exploit their synergistic relationships develops catalytic, electronic, optical, and magnetic properties that are superior to those of monometallic NPs [108].

In the synthesis process, bimetallic systems can produce different types of nanostructures, microscopically in the form of alloys or core/shell structures, whose properties are controlled by varying the molar ratios of the constituent metals. For example, Au–Ag bimetallic nanoparticles, produced by green methods involving fruit juice extracts, have been reported to be excellent catalysts for the reduction in nitrophenols and the degradation of organic dyes. Moreover, their capacity to enhance the thermal conductivity of alkali fluid and exhibit prominent antioxidant activity will open up broader opportunities in the field of functional nanofluids and biomedicine [109].

Amino Acid-Functionalized Bimetallic Au–Ag NPs

Du and co-workers proposed a novel method for the detection of Cd(II) in water, using Au–Ag NPs functionalized with *L-cysteine*. Bimetallic nanoparticles are synthesized by reducing $HAuCl_4$ and $AgNO_3$ in aqueous solution and then functionalizing them with *L-cysteine* [110]. When Cd(II) is present, it induces the aggregation of the functionalized Au–Ag NPs, simultaneously resulting in a visible color transition of the suspension from orange-yellow to green, which can be followed by UV-Vis spectroscopy. This method is simple, selective, and sensitive, justifying its prospective implementation in the analysis of raw water environments (Table 5). Bimetallic nanoparticles such as Au/Ag have been reported to be of interest because gold and silver can potentially form alloys due to

their nearly similar crystal lattice constants, offering better properties than monometallic nanoparticles [110].

Another study has revealed a relatively short peptide of six AAs capable of directly converting Au(III) or Ag(I) ions to nanoscale by reduction, while simultaneously stabilizing them as capping agents under ambient conditions [80]. The authors also addressed the dissolution of peptide-capped gold and silver nanoparticles for pH-dependent detection of HMs such as Hg(II), Mn(II), and Fe(II) based on absorbance changes. The studies further addressed bimetallic nanoparticles by demonstrating the formation of core/shell Au–Ag nanoparticles. Gold nanoparticles are coated with a silver shell through peptide-mediated photoreduction. These bimetallic Au–Ag core/shell nanoparticles were analyzed using UV-Vis spectroscopy, high-resolution scanning transmission electron microscopy (HR-STEM), and energy-dispersive X-ray spectroscopy (EDS). The study focuses on the use of this novel peptide in the one-step, one-pot synthesis and stabilization of AuNPs, AgNPs, and Au–Ag core/shell nanoparticles, with selective detection of different metal ions. The study also highlights the advantage of bimetallic nanoparticles, which combine the properties of both the core and shell materials. Au–Ag core/shell nanoparticles benefit from the stability of AuNPs and the high surface plasmon band density of AgNPs, making them useful for colorimetric or spectroscopic detection.

Table 5. Bimetallic nanoparticles properties and applications.

Characteristic	Au–Ag (Green Synthesis) [109]	Au–Ag (*L-cysteine* Functionalized) [110]	Au–Ag (Protein-Mediated Core/Shell) [80]
Synthesis method	Green method involving fruit juice of pomegranate	Reduction in $HAuCl_4$ and $AgNO_3$, functionalized with *L-cysteine*	Peptide-mediated photoreduction
Application	Catalysis, nanofluids, biomedicine	Cd(II) detection in water	Colorimetric or spectroscopic detection of metal ions
Properties	Excellent catalysts, enhanced thermal conductivity, antioxidant activity	Aggregation upon Cd(II) presence, color transition	Stability of AuNPs, high surface plasmon band density of AgNPs

5. Conclusions

This review reflects the growing interest in the application of amino acid-modified AuNPs and AgNPs in the detection and removal of various HMs from the environment. Studies show that incorporating Au and Ag NPs with different AA moieties improve their stability and reusability, extending their lifespan to several months and cycles, as well as their biocompatibility in diverse real-world environmental applications, such as wastewater and soil remediation. Au and Ag NPs can bind to various functional groups of the AAs, such as carboxyl, amine and thiol. Furthermore, AAs can act as reducing or stabilizing agents, preventing nanoparticle aggregation and thus increasing their effectiveness over extended periods. Furthermore, this review indicates the potential for easily monitoring and measuring the effectiveness of AA-functionalized Au/AgNP complexes in detecting and binding various heavy metals using diverse electrochemical and optical detection techniques. These complexes exhibit high sensitivity and efficiency in detecting a wide range of heavy metals. Therefore, this review highlights the potential of processing, applying and reusing functionalized amino acid NPs in detecting and removing heavy metal contamination, emphasizing the use of advanced, low-cost, sustainable and environmentally friendly synthesis and deployment methods. Furthermore, integrating future computational studies on the binding of these complexes to heavy metal ions will enhance researchers' understanding of the types of binding, structural changes, energy variations, and stability of these bonds. Current research on AA-functionalized nanoparticles holds

promising potential for advancing scientific research, environmental sustainability and public health. Continued research into their applications can lead to innovative solutions for combating heavy metal pollution and protecting ecosystems from its destructive effects.

Author Contributions: Conceptualization, G.S.K.; resources, R.M.E. and G.S.K.; writing—original draft preparation, R.M.E. and G.S.K.; writing—review and editing, I.U.H.B., S.A.R. and A.N.; supervision, G.S.K.; project administration, G.S.K.; funding acquisition, A.N. All authors have read and agreed to the published version of the manuscript.

Funding: This work was supported by the Deanship of Scientific Research, Vice Presidency for Graduate Studies and Scientific Research, King Faisal University, Saudi Arabia [Grant No. KFU262348].

Institutional Review Board Statement: Not applicable.

Informed Consent Statement: Not applicable.

Data Availability Statement: No new data were created or analyzed in this study. Data sharing is not applicable to this article.

Conflicts of Interest: The authors declare no conflicts of interest.

References

1. Vandenbossche, M.; Jimenez, M.; Casetta, M.; Traisnel, M. Remediation of heavy metals by biomolecules: A review. *Crit. Rev. Environ. Sci. Technol.* **2015**, *45*, 1644–1704. [CrossRef]
2. Hou, T.; Yu, S.; Zhou, M.; Wu, M.; Liu, J.; Zheng, X.; Li, J.; Wang, J.; Wang, X. Effective removal of inorganic and organic heavy metal pollutants with poly (amino acid)-based micromotors. *Nanoscale* **2020**, *12*, 5227–5232. [CrossRef]
3. Liu, X.; Wu, M.; Li, C.; Yu, P.; Feng, S.; Li, Y.; Zhang, Q. Interaction structure and affinity of zwitterionic amino acids with important metal cations (Cd^{2+}, Cu^{2+}, Fe^{3+}, Hg^{2+}, Mn^{2+}, Ni^{2+} and Zn^{2+}) in aqueous solution: A theoretical study. *Molecules* **2022**, *27*, 2407. [CrossRef] [PubMed]
4. Caporale, A.G.; Violante, A. Chemical processes affecting the mobility of heavy metals and metalloids in soil environments. *Curr. Pollut. Rep.* **2016**, *2*, 15–27. [CrossRef]
5. Ahmad, W.; Alharthy, R.D.; Zubair, M.; Ahmed, M.; Hameed, A.; Rafique, S. Toxic and heavy metals contamination assessment in soil and water to evaluate human health risk. *Sci. Rep.* **2021**, *11*, 17006. [CrossRef]
6. Selvi, A.; Rajasekar, A.; Theerthagiri, J.; Ananthaselvam, A.; Sathishkumar, K.; Madhavan, J.; Rahman, P.K. Integrated remediation processes toward heavy metal removal/recovery from various environments—A review. *Front. Environ. Sci.* **2019**, *7*, 66. [CrossRef]
7. Aziz, K.H.H.; Mustafa, F.S.; Omer, K.M.; Hama, S.; Hamarawf, R.F.; Rahman, K.O. Heavy metal pollution in the aquatic environment: Efficient and low-cost removal approaches to eliminate their toxicity: A review. *RSC Adv.* **2023**, *13*, 17595–17610. [CrossRef]
8. Jin, M.; Yuan, H.; Liu, B.; Peng, J.; Xu, L.; Yang, D. Review of the distribution and detection methods of heavy metals in the environment. *Anal. Methods* **2020**, *12*, 5747–5766. [CrossRef] [PubMed]
9. Punia, P.; Bharti, M.K.; Dhar, R.; Thakur, P.; Thakur, A. Recent advances in detection and removal of heavy metals from contaminated water. *ChemBioEng Rev.* **2022**, *9*, 351–369. [CrossRef]
10. Buledi, J.A.; Amin, S.; Haider, S.I.; Bhanger, M.I.; Solangi, A.R. A review on detection of heavy metals from aqueous media using nanomaterial-based sensors. *Environ. Sci. Pollut. Res.* **2021**, *28*, 58994–59002. [CrossRef]
11. Li, M.; Shi, Q.; Song, N.; Xiao, Y.; Wang, L.; Chen, Z.; James, T.D. Current trends in the detection and removal of heavy metal ions using functional materials. *Chem. Soc. Rev. Reso* **2023**, *52*, 5827–5860. [CrossRef]
12. Malik, L.A.; Bashir, A.; Qureashi, A.; Pandith, A.H. Detection and removal of heavy metal ions: A review. *Environ. Chem. Lett.* **2019**, *17*, 1495–1521. [CrossRef]
13. Altammar, K.A. A review on nanoparticles: Characteristics, synthesis, applications, and challenges. *Front. Microbiol.* **2023**, *14*, 1155622. [CrossRef] [PubMed]
14. De Silva, M.; Cao, G.; Tam, K.C. Nanomaterials for the removal and detection of heavy metals: A review. *Environ. Sci. Nano* **2025**, *12*, 2154–2176. [CrossRef]
15. Kus-Liśkiewicz, M.; Fickers, P.; Ben Tahar, I. Biocompatibility and cytotoxicity of gold nanoparticles: Recent advances in methodologies and regulations. *Int. J. Mol. Sci.* **2021**, *22*, 10952. [CrossRef]

16. Sati, A.; Ranade, T.N.; Mali, S.N.; Ahmad Yasin, H.K.; Pratap, A. Silver nanoparticles (AgNPs): Comprehensive insights into bio/synthesis, key influencing factors, multifaceted applications, and toxicity—A 2024 update. *ACS Omega* **2025**, *10*, 7549–7582. [CrossRef]
17. Ujica, M.A.; Paltinean, G.A.; Mocanu, A.; Tomoaia-Cotisel, M. Silver and gold nanoparticles: Challenges and perspectives. *Acad. Rom. Sci. Ann.-Ser. Biol. Sci.* **2020**, *9*, 97–139. [CrossRef]
18. Pušnik, K.; Peterlin, M.; Cigić, I.K.; Marolt, G.; Kogej, K.; Mertelj, A.; Gyergyek, S.O.; Makovec, D. Adsorption of amino acids, aspartic acid, and lysine onto iron-oxide nanoparticles. *J. Phys. Chem. C* **2016**, *120*, 14372–14381. [CrossRef]
19. Buglak, A.A.; Kononov, A.I. Comparative study of gold and silver interactions with amino acids and nucleobases. *RSC Adv.* **2020**, *10*, 34149–34160. [CrossRef]
20. Madhavan, A.A.; Qotainy, R.; Nair, R. Synthesis of functionalized silver nanoparticles and its application as chemical sensor. In *2019 Advances in Science and Engineering Technology International Conferences (ASET)*; IEEE: New York, NY, USA, 2019; pp. 1–4.
21. Sener, G.; Uzun, L.; Denizli, A. Colorimetric sensor array based on gold nanoparticles and amino acids for identification of toxic metal ions in water. *ACS Appl. Mater. Interfaces* **2014**, *6*, 18395–18400. [CrossRef]
22. Zhang, X.; Zhang, Y.; Gu, Y.; Zhou, J.; Li, M.; Qi, J. A Naked-Eye Colorimetric Ratio Method for the Selective and Sensitive Detection of L-Cys Based on a Silver Nanoflakes–Chromium (III) Ion System. *Chemosensors* **2024**, *12*, 80. [CrossRef]
23. Gluhar, S.; Kaurin, A.; Lestan, D. Soil washing with biodegradable chelating agents and EDTA: Technological feasibility, remediation efficiency and environmental sustainability. *Chemosphere* **2020**, *257*, 127226. [CrossRef] [PubMed]
24. Dolev, N.; Katz, Z.; Ludmer, Z.; Ullmann, A.; Brauner, N.; Goikhman, R. Natural amino acids as potential chelators for soil remediation. *Environ. Res.* **2020**, *183*, 109140. [CrossRef]
25. Yao, W.; Yang, Z.; Huang, L.; Su, C. Complexation of amino acids with cadmium and their application for cadmium-contaminated soil remediation. *Appl. Sci.* **2022**, *12*, 1114. [CrossRef]
26. Plohl, O.; Simonič, M.; Kolar, K.; Gyergyek, S.; Fras Zemljič, L. Magnetic nanostructures functionalized with a derived lysine coating applied to simultaneously remove heavy metal pollutants from environmental systems. *Sci. Technol. Adv. Mater.* **2021**, *22*, 55–71. [CrossRef]
27. Vandenbossche, M.; Dehaese, A.; Casetta, M.; Jimenez, M.; Traisnel, M. Tyrosine: An efficient natural molecule for copper remediation. *Green Mater.* **2015**, *3*, 1–9. [CrossRef]
28. Sarkodie, E.K.; Li, K.; Guo, Z.; Yang, J.; Deng, Y.; Shi, J.; Peng, Y.; Jiang, Y.; Jiang, H.; Liu, H. The Effect of Cysteine on the Removal of Cadmium in Paddy Soil by Combination with Bioremediation and the Response of the Soil Microbial Community. *Toxics* **2024**, *13*, 22. [CrossRef]
29. Bansal, M.; Ram, B.; Chauhan, G.S.; Kaushik, A. *L-cysteine* functionalized bagasse cellulose nanofibers for mercury (II) ions adsorption. *Int. J. Biol. Macromol.* **2018**, *112*, 728–736. [CrossRef] [PubMed]
30. Tsai, S.-Y.; Chang, C.-K.; Wei, P.-Y.; Huang, S.-Y.; Gavahian, M.; Santoso, S.P.; Hsieh, C.-W. Effective removal of different heavy metals ion (Cu, Pb, and Cd) from aqueous solutions by various molecular weight and salt types of poly-γ-glutamic acid. *Molecules* **2024**, *29*, 1054. [CrossRef] [PubMed]
31. Ogunleye, A.; Bhat, A.; Irorere, V.U.; Hill, D.; Williams, C.; Radecka, I. Poly-γ-glutamic acid: Production, properties and applications. *Microbiology* **2015**, *161*, 1–17. [CrossRef] [PubMed]
32. Syeda, H.I.; Muthukumaran, S.; Baskaran, K. Polyglutamic acid and its derivatives as multi-functional biopolymers for the removal of heavy metals from water: A review. *J. Water Process Eng.* **2023**, *56*, 104367. [CrossRef]
33. Song, Y.; Zhan, J.; Li, M.; Zhao, H.; Shi, G.; Wu, M.; Fang, H. Enhancement of the water affinity of histidine by zinc and copper ions. *Int. J. Mol. Sci.* **2022**, *23*, 3957. [CrossRef]
34. Remelli, M.; Nurchi, V.M.; Lachowicz, J.I.; Medici, S.; Zoroddu, M.A.; Peana, M. Competition between Cd(II) and other divalent transition metal ions during complex formation with amino acids, peptides, and chelating agents. *Coord. Chem. Rev.* **2016**, *327–328*, 55–69. [CrossRef]
35. Allwin Mabes Raj, A.; Bauman, M.; Lakić, M.; Dimitrušev, N.; Lobnik, A.; Košak, A. Removal of Pb^{2+}, CrT, and Hg^{2+} ions from aqueous solutions using amino-functionalized magnetic nanoparticles. *Int. J. Mol. Sci.* **2022**, *23*, 16186. [CrossRef]
36. Youssif, M.M.; El-Attar, H.G.; Hessel, V.; Wojnicki, M. Recent Developments in the Adsorption of Heavy Metal Ions from Aqueous Solutions Using Various Nanomaterials. *Materials* **2024**, *17*, 5141. [CrossRef]
37. Ivaska, A. Electrochemical detection. In *Comprehensive Analytical Chemistry*; Elsevier: Amsterdam, The Netherlands, 2008; Volume 54, pp. 441–459.
38. Li, Z.; Zhu, M. Detection of pollutants in water bodies: Electrochemical detection or photo-electrochemical detection? *Chem. Commun.* **2020**, *56*, 14541–14552. [CrossRef]
39. Chen, S.H.; Li, Y.X.; Li, P.H.; Xiao, X.Y.; Jiang, M.; Li, S.S.; Zhou, W.Y.; Yang, M.; Huang, X.J.; Liu, W.Q. Electrochemical spectral methods for trace detection of heavy metals: A review. *TrAC Trends Anal. Chem.* **2018**, *106*, 139–150. [CrossRef]
40. Ajay Piriya, V.S.; Printo, J.; Kiruba Daniel, S.G.G.; Susithra, L.; Takatoshi, K.; Sivakumar, M. Colorimetric sensors for rapid detection of various analytes. *Mater. Sci. Eng. C* **2017**, *78*, 1231–1245. [CrossRef] [PubMed]

41. Bhat, A.; Tian, F.; Singh, B. Advances in na-nomaterials and colorimetric detection of arsenic in water: Review and future perspectives. *Sensors* **2024**, *24*, 3889. [CrossRef]
42. Niu, H.; Liu, J.; O'Connor, H.M.; Gunnlaugsson, T.; James, T.D.; Zhang, H. Photoinduced electron transfer (PeT) based fluorescent probes for cellular imaging and disease therapy. *Chem. Soc. Rev.* **2023**, *52*, 2322–2357. [CrossRef]
43. Nugent, J.W.; Lee, H.; Lee, H.S.; Reibenspies, J.H.; Hancock, R.D. Mechanism of chelation enhanced fluorescence in complexes of cadmium (ii), and a possible new type of anion sensor. *Chem. Commun.* **2013**, *49*, 9749–9751. [CrossRef]
44. Clegg, R.M. Fluorescence resonance energy transfer. *Curr. Opin. Biotechnol.* **1995**, *6*, 103–110. [CrossRef]
45. Hong, Y.; Lam, J.W.; Tang, B.Z. Aggregation-induced emission. *Chem. Soc. Rev.* **2011**, *40*, 5361–5388. [CrossRef]
46. Hong, Y.; Lam, J.W.; Tang, B.Z. Aggregation-induced emission: Phenomenon, mechanism and applications. *Chem. Commun.* **2009**, *29*, 4332–4353. [CrossRef] [PubMed]
47. Siraj, N.; El-Zahab, B.; Hamdan, S.; Karam, T.E.; Haber, L.H.; Li, M.; Fakayode, S.O.; Das, S.; Valle, B.; Strongin, R.M.; et al. Fluorescence, phosphorescence, and chemiluminescence. *Anal. Chem.* **2016**, *88*, 170–202. [CrossRef]
48. Chen, Y.; Ming, H. Review of surface plasmon resonance and localized surface plasmon resonance sensor. *Photonic Sens.* **2012**, *2*, 37–49. [CrossRef]
49. Mayer, K.M.; Hafner, J.H. Localized surface plasmon resonance sensors. *Chem. Rev.* **2011**, *111*, 3828–3857. [CrossRef]
50. Butt, M.A.; Voronkov, G.S.; Grakhova, E.P.; Kutluyarov, R.V.; Kazanskiy, N.L.; Khonina, S.N. Environmental monitoring: A comprehensive review on optical waveguide and fiber-based sensors. *Biosensors* **2022**, *12*, 1038. [CrossRef] [PubMed]
51. Dakin, J.P.; Hotate, K.; Lieberman, R.A.; Marcus, M.A. Optical fiber sensors. In *Handbook of Optoelectronics*, 2nd ed.; Taylor and Francis: Abingdon, UK, 2017; pp. 347–430.
52. Rai, A.; Seena, S.; Gagliardi, T.; Palma, P.J. Advances in the design of amino acid and peptide synthesized gold nanoparticles for their applications. *Adv. Colloid Interface Sci.* **2023**, *318*, 102951. [CrossRef] [PubMed]
53. Zong, J.; Cobb, S.L.; Cameron, N.R. Peptide-functionalized gold nanoparticles: Versatile biomaterials for diagnostic and therapeutic applications. *Biomater. Sci.* **2017**, *5*, 872–886. [CrossRef] [PubMed]
54. Zhang, G. Functional gold nanoparticles for sensing applications. *Nanotechnol. Rev.* **2013**, *2*, 269–288. [CrossRef]
55. Hyder, A.; Buledi, J.A.; Nawaz, M.; Rajpar, D.B.; Shah, Z.-u.-H.; Orooji, Y.; Yola, M.L.; Karimi-Maleh, H.; Lin, H.; Solangi, A.R. Identification of heavy metal ions from aqueous environment through gold, Silver and Copper Nanoparticles: An excellent colorimetric approach. *Environ. Res.* **2022**, *205*, 112475. [CrossRef] [PubMed]
56. Priyadarshini, E.; Pradhan, N. Gold nanoparticles as efficient sensors in colorimetric detection of toxic metal ions: A review. *Sens. Actuators B Chem.* **2017**, *238*, 888–902. [CrossRef]
57. Havaldar, D.V.; Patil, R.V.; Moholkar, D.N.; Magdum, P.S.; Vadrale, A.P.; Pawar, K.D. Differently synthesized gold nanoparticles respond differently to functionalization with *L*-amino acids. *Particuology* **2020**, *52*, 97–104. [CrossRef]
58. Shao, Q.; Hall, C.K. Binding preferences of amino acids for gold nanoparticles: A molecular simulation study. *Langmuir* **2016**, *32*, 7888–7896. [CrossRef]
59. Zare, D.; Khoshnevisan, K.; Barkhi, M.; Tahami, H.V. Fabrication of capped gold nanoparticles by using various amino acids. *J. Exp. Nanosci.* **2014**, *9*, 957–965. [CrossRef]
60. Maruyama, T.; Fujimoto, Y.; Maekawa, T. Synthesis of gold nanoparticles using various amino acids. *J. Colloid Interface Sci.* **2015**, *447*, 254–257. [CrossRef]
61. Hamaguchi, K.; Kawasaki, H.; Arakawa, R. Photochemical synthesis of glycine-stabilized gold nanoparticles and its heavy-metal-induced aggregation behavior. *Colloids Surf. A Physicochem. Eng. Asp.* **2010**, *367*, 167–173. [CrossRef]
62. Aryal, S.; Remant, B.; Dharmaraj, N.; Bhattarai, N.; Kim, C.H.; Kim, H.Y. Spectroscopic identification of SAu interaction in cysteine capped gold nanoparticles. *Spectrochim. Acta Mol. Biomol. Spectrosc.* **2006**, *63*, 160–163. [CrossRef]
63. Grosan, C.B.; Varodi, C.; Vulcu, A.; Olenic, L.; Pruneanu, S.; Almasan, V. Structural and electrochemical characterization of novel leucine–gold nanoparticles modified electrode. *Electrochim. Acta* **2012**, *63*, 146–152. [CrossRef]
64. Ly, N.H.; Oh, C.H.; Joo, S.-W. A submicromolar Cr(III) sensor with a complex of methionine using gold nanoparticles. *Sens. Actuators B Chem.* **2015**, *219*, 276–282. [CrossRef]
65. Sang, F.; Li, X.; Zhang, Z.; Liu, J.; Chen, G. Recyclable colorimetric sensor of Cr^{3+} and Pb^{2+} ions simultaneously using a zwitterionic amino acid modified gold nanoparticles. *Spectrochim. Acta Mol. Biomol. Spectrosc.* **2018**, *193*, 109–116. [CrossRef]
66. Annadhasan, M.; Muthukumarasamyvel, T.; Sankar Babu, V.; Rajendiran, N. Green synthesized silver and gold nanoparticles for colorimetric detection of Hg^{2+}, Pb^{2+}, and Mn^{2+} in aqueous medium. *ACS Sustain. Chem. Eng.* **2014**, *2*, 887–896. [CrossRef]
67. Wang, X.; Wang, X.; Liu, J.; Wang, K.; Zhao, R.; Yang, S. Ingenious aspartic acid-functionalized gold nanoparticles by one-pot protocol for the sensitive detection of chromium(III) ions. *Microchem. J.* **2020**, *159*, 105359. [CrossRef]
68. Eviane, D.; Siswanta, D.; Santosa, S.J. pH Dependence on Colorimetric Detection of Hg^{2+} by Histidine-Functionalized Gold Nanoparticles. *Indones. J. Chem.* **2020**, *20*, 941–952. [CrossRef]
69. Liu, Z.; Yan, Y.; Li, J.; Zhou, W.; Gao, H.; Lu, R. Rapid visual dual-mode detection of Zr(IV) based on l-histidine functionalized gold nanoparticles. *Anal. Sci.* **2024**, *40*, 1269–1278. [CrossRef]

70. Sener, G.; Uzun, L.; Denizli, A. Lysine-promoted colorimetric response of gold nanoparticles: A simple assay for ultrasensitive mercury(II) detection. *Anal. Chem.* **2014**, *86*, 514–520. [CrossRef] [PubMed]
71. Wang, J.; Bian, C.; Tong, J.; Sun, J.; Xia, S. *L*-Aspartic acid/*L-cysteine*/gold nanoparticle modified microelectrode for simultaneous detection of copper and lead. *Thin Solid Films* **2012**, *520*, 6658–6663. [CrossRef]
72. Zhuo, Y.; Liang, J.; Chen, X.; Luo, J.; Huang, Z.; Zheng, F.; Liu, F.; Li, S. Methionine and cysteine modified AuNPs@ PVP as high stable, selective and anti-interference colorimetric sensor for the detection of Cu^{2+} and Hg^{2+} in urine and serum. *Microchem. J.* **2025**, *209*, 112849. [CrossRef]
73. Liu, Z.; Zu, Y.; Fu, Y.; Meng, R.; Guo, S.; Xing, Z.; Tan, S. Hydrothermal synthesis of histidine-functionalized single-crystalline gold nanoparticles and their pH-dependent UV absorption characteristic. *Colloids Surf. B Biointerfaces* **2010**, *76*, 311–316. [CrossRef] [PubMed]
74. Boas, D.; Remennik, S.; Reches, M. Peptide-capped Au and Ag nanoparticles: Detection of heavy metals and photochemical core/shell formation. *J. Colloid Interface Sci.* **2023**, *631*, 66–76. [CrossRef]
75. Nowinski, A.K.; White, A.D.; Keefe, A.J.; Jiang, S. Biologically inspired stealth peptide-capped gold nanoparticles. *Langmuir* **2014**, *30*, 1864–1870. [CrossRef]
76. Khoshnevisan, K.; Daneshpour, M.; Barkhi, M.; Gholami, M.; Samadian, H.; Maleki, H. The promising potentials of capped gold nanoparticles for drug delivery systems. *J. Drug Target.* **2018**, *26*, 525–532. [CrossRef] [PubMed]
77. Briggs, B.D.; Li, Y.; Swihart, M.T.; Knecht, M.R. Reductant and sequence effects on the morphology and catalytic activity of peptide-capped Au nanoparticles. *ACS Appl. Mater. Interfaces* **2015**, *7*, 8843–8851. [CrossRef] [PubMed]
78. Chen, G.; Xie, Y.; Peltier, R.; Lei, H.; Wang, P.; Chen, J.; Hu, Y.; Wang, F.; Yao, X.; Sun, H. Peptide-decorated gold nanoparticles as functional nano-capping agent of mesoporous silica container for targeting drug delivery. *ACS Appl. Mater. Interfaces* **2016**, *8*, 11204–11209. [CrossRef]
79. Song, M.; Sun, Y.; Luo, Y.; Zhu, Y.; Liu, Y.; Li, H. Exploring the mechanism of inhibition of au nanoparticles on the aggregation of amyloid-β (16-22) peptides at the atom level by all-atom molecular dynamics. *Int. J. Mol. Sci.* **2018**, *19*, 1815. [CrossRef]
80. Nguyen, M.A.; Hughes, Z.E.; Liu, Y.; Li, Y.; Swihart, M.T.; Knecht, M.R.; Walsh, T.R. Peptide-mediated growth and dispersion of Au nanoparticles in water via sequence engineering. *J. Phys. Chem. C* **2018**, *122*, 11532–11542. [CrossRef]
81. Yu, J.; Becker, M.; Carri, G.A. A molecular dynamics simulation of the stability-limited growth mechanism of peptide-mediated gold-nanoparticle synthesis. *Small* **2010**, *6*, 2242. [CrossRef]
82. Brancolini, G.; Bellucci, L.; Maschio, M.C.; Di Felice, R.; Corni, S. The interaction of peptides and proteins with nanostructures surfaces: A challenge for nanoscience. *Curr. Opin. Colloid Interface Sci.* **2019**, *41*, 86–94. [CrossRef]
83. Erdoğan, H. Colorimetric Determination of Cu^{2+} by Glycine-Histidine Dipeptide Functionalized-Gold Nanoparticles. *Duzce Univ. J. Sci. Technol.* **2021**, *9*, 1469–1482. [CrossRef]
84. Gunupuru, R.; Maity, D.; Vyas, G.; Paul, P. Water dispersible glycylglycine functionalized gold nanoparticles: Application in colorimetric sensing of Hg(II), Pb(II) and Cr(III) in aqueous media. *J. Chem. Sci.* **2022**, *134*, 80. [CrossRef]
85. Yang, Z.; Lyu, J.; Qian, J.; Wang, Y.; Liu, Z.; Yao, Q.; Chen, T.; Cao, Y.; Xie, J. Glutathione: A naturally occurring tripeptide for functional metal nanomaterials. *Chem. Sci.* **2025**, *16*, 6542–6572. [CrossRef]
86. Fernández-Ponce, C.; Mánuel, J.; Fernández-Cisnal, R.; Félix, E.; Beato-López, J.; Munoz-Miranda, J.; Beltrán, A.; Santos, A.; Morales, F.; Yeste, M. Superficial characteristics and functionalization effectiveness of non-toxic glutathione-capped magnetic, fluorescent, metallic and hybrid nanoparticles for biomedical applications. *Metals* **2021**, *11*, 383. [CrossRef]
87. Flowers, J.A.; Farrell, M.J.; Rutherford, G.; Pradhan, A.K. Colorimetric and label-free optical detection of Pb^{2+} ions via colloidal gold nanoparticles. *Biosensors* **2023**, *13*, 819. [CrossRef]
88. Jiang, M.; Chen, H.-R.; Li, S.-S.; Liang, R.; Liu, J.-H.; Yang, Y.; Wu, Y.-J.; Yang, M.; Huang, X.-J. The selective capture of Pb^{2+} in rice phloem sap using glutathione-functionalized gold nanoparticles/multi-walled carbon nanotubes: Enhancing anti-interference electrochemical detection. *Environ. Sci. Nano* **2018**, *5*, 2761–2771. [CrossRef]
89. Guo, Y.; Wang, Z.; Qu, W.; Shao, H.; Jiang, X. Colorimetric detection of mercury, lead and copper ions simultaneously using protein-functionalized gold nanoparticles. *Biosens. Bioelectron.* **2011**, *26*, 4064–4069. [CrossRef]
90. Nadumane, S.S.; Biswas, R.; Mazumder, N. Eco-friendly colorimetric detection of lead and mercury using *L-cysteine*-functionalized gold nanoparticles: A step towards greening the exposome. *RSC Adv.* **2025**, *15*, 11573–11579. [CrossRef] [PubMed]
91. Seth, R. *L-cysteine* functionalized gold nanoparticles as a colorimetric sensor for ultrasensitive detection of toxic metal ion cadmium. *Mater. Today Proc.* **2020**, *24*, 2375–2382.
92. Jijana, A.N.; Mphuthi, N.; Shumbula, P.; Vilakazi, S.; Sikhwivhilu, L. The ultra-sensitive electrochemical detection of As(III) in ground water using disposable *L-cysteine*/Lipoic Acid functionalised gold nanoparticle modified screen-printed electrodes. *Electrocatalysis* **2021**, *12*, 310–325. [CrossRef]
93. Khavani, M.; Mehranfar, A.; Izadyar, M. A theoretical approach on the ability of functionalized gold nanoparticles for detection of Cd^{2+}. *Sci. Rep.* **2021**, *11*, 23422. [CrossRef] [PubMed]

94. Oliveira, E.; Nunez, C.; Rodriguez-Gonzalez, B.; Capelo, J.L.; Lodeiro, C. Novel small stable gold nanoparticles bearing fluorescent cysteine–coumarin probes as new metal-modulated chemosensors. *Inorg. Chem.* **2011**, *50*, 8797–8807. [CrossRef]
95. Atapour, M.; Amoabediny, G.; Ahmadzadeh-Raji, M. Integrated optical and electrochemical detection of Cu^{2+} ions in water using a sandwich amino acid–gold nanoparticle-based nano-biosensor consisting of a transparent-conductive platform. *RSC Adv.* **2019**, *9*, 8882–8893. [CrossRef]
96. Abou El-Nour, K.M.; Eftaiha, A.A.; Al-Warthan, A.; Ammar, R.A. Synthesis and applications of silver nanoparticles. *Arab. J. Chem.* **2010**, *3*, 135–140. [CrossRef]
97. Khodashenas, B.; Ghorbani, H.R. Synthesis of silver nanoparticles with different shapes. *Arab. J. Chem.* **2019**, *12*, 1823–1838. [CrossRef]
98. Janani, B.; Syed, A.; Raju, L.L.; Marraiki, N.; Elgorban, A.M.; Zaghloul, N.S.; Thomas, A.M.; Das, A.; Khan, S.S. Highly selective and effective environmental mercuric ion detection method based on starch modified Ag NPs in presence of glycine. *Opt. Commun.* **2020**, *465*, 125564. [CrossRef]
99. Burratti, L.; Bertelà, F.; Sisani, M.; Di Guida, I.; Battocchio, C.; Iucci, G.; Prosposito, P.; Venditti, I. Three-Dimensional Printed Filters Based on Poly(ethylene glycol) Diacrylate Hydrogels Doped with Silver Nanoparticles for Removing Hg(II) Ions from Water. *Polymers* **2024**, *16*, 1034. [CrossRef]
100. Kannaiyan, S.; Gopal, A.; Lakshmipathy, R.; Ali, D.; Alarifi, S.; Geetha, M.; Sadasivuni, K.K. Glycine-modified chitosan-embedded silver nanoparticles: A green approach to Pb^{2+} adsorption and bioactivity enhancement. *Chem. Pap.* **2025**, *79*, 1087–1101. [CrossRef]
101. Hosseini, S.; Aghaie, H.; Ghaedi, M.; Dashtian, K.; Purkait, M. Lead(II) adsorption from aqueous solutions onto modified ag nanoparticles: Modeling and optimization. *Environ. Prog. Sustain. Energy* **2016**, *35*, 743–749. [CrossRef]
102. Samuel, V.R.; Rao, K.J. A rapid colorimetric dual sensor for the detection of mercury and lead ions in water using cysteine capped silver nanoparticles. *Chem. Phys. Impact* **2023**, *6*, 100161. [CrossRef]
103. Balasurya, S.; Syed, A.; Thomas, A.M.; Marraiki, N.; Elgorban, A.M.; Raju, L.L.; Das, A.; Khan, S.S. Rapid colorimetric detection of mercury using silver nanoparticles in the presence of methionine. *Spectrochim. Acta Part A Mol. Biomol. Spectrosc.* **2020**, *228*, 117712. [CrossRef] [PubMed]
104. Contino, A.; Maccarrone, G.; Zimbone, M.; Reitano, R.; Musumeci, P.; Calcagno, L.; Oliveri, I.P. Tyrosine capped silver nanoparticles: A new fluorescent sensor for the quantitative determination of copper(II) and cobalt(II) ions. *J. Colloid Interface Sci.* **2016**, *462*, 216–222. [CrossRef] [PubMed]
105. Liu, Z.; Xing, Z.; Zu, Y.; Tan, S.; Zhao, L.; Zhou, Z.; Sun, T. Synthesis and characterization of *L*-histidine capped silver nanoparticles. *Mater. Sci. Eng. C* **2012**, *32*, 811–816. [CrossRef]
106. Zhu, J.; Zhang, H.; Chen, R.; Liu, Q.; Liu, J.; Yu, J.; Li, R.; Zhang, M.; Wang, J. An anti-algae adsorbent for uranium extraction: L-Arginine functionalized graphene hydrogel loaded with Ag nanoparticles. *J. Colloid Interface Sci.* **2019**, *543*, 192–200. [CrossRef]
107. Buduru, P.; Reddy, B.S.R.; Naidu, N. Functionalization of silver nanoparticles with glutamine and histidine for simple and selective detection of Hg^{2+} ion in water samples. *Sens. Actuators B Chem.* **2017**, *244*, 972–982. [CrossRef]
108. Dlamini, N.G.; Basson, A.K.; Pullabhotla, V.S.R. Synthesis and characterization of various bimetallic nanoparticles and their application. *Appl. Nano* **2023**, *4*, 1–24. [CrossRef]
109. Kumari, M.M.; Jacob, J.; Philip, D. Green synthesis and applications of Au–Ag bimetallic nanoparticles. *Spectrochim. Acta Part A Mol. Biomol. Spectrosc.* **2015**, *137*, 185–192. [CrossRef]
110. Du, J.; Hu, X.; Zhang, G.; Wu, X.; Gong, D. Colorimetric detection of cadmium in water using *L-cysteine* functionalized gold–silver nanoparticles. *Anal. Lett.* **2018**, *51*, 2906–2919. [CrossRef]

Disclaimer/Publisher's Note: The statements, opinions and data contained in all publications are solely those of the individual author(s) and contributor(s) and not of MDPI and/or the editor(s). MDPI and/or the editor(s) disclaim responsibility for any injury to people or property resulting from any ideas, methods, instructions or products referred to in the content.